Title: Protein Quality Control is a Risk Factor and Therapeutic Target in Toxin-Induced Biliary Atresia

One Sentence Summary: Protein quality control plays an evolutionarily conserved role in cholangiocyte injury responses and is a novel therapeutic target for biliary disease.

Authors: Xiao Zhao[1], Kristin Lorent[1], Diana Escobar-Zarate[1], Ramakrishnan Rajagopalan[2], Kathleen M. Loomes[3], Kevin Gillespie[4], Clementina Mesaros[4], Michelle A. Estrada[5], Ian Blair[4], Jeffrey D. Winkler[5], Nancy B. Spinner[3], Marcella Devoto[6,7,8], Michael Pack[1,9]*

Affiliations:

[1]Division of Gastroenterology, Department of Medicine, Perelman School of Medicine, University of Pennsylvania, Philadelphia, PA, USA.

[2]Division of Genomic Diagnostics, Department of Pathology, The Children's Hospital of Philadelphia and University of Pennsylvania Perelman School of Medicine, Philadelphia, PA, USA.

[3]Division of Gastroenterology, Hepatology and Nutrition, Department of Pediatrics, The Children's Hospital of Philadelphia and University of Pennsylvania Perelman School of Medicine, Philadelphia, PA, USA.

[4]Department of System Pharmacology and Translational Therapeutics, Perelman School of Medicine, University of Pennsylvania, Philadelphia, PA, USA.

[5]Department of Chemistry, University of Pennsylvania, Philadelphia, PA, USA.

[6]Division of Human Genetics, Children's Hospital of Philadelphia, Philadelphia, PA, USA.

[7]Departments of Pediatrics and of Biostatistics, Epidemiology and Informatics, Perelman School of Medicine, University of Pennsylvania, Philadelphia, PA, USA.

[8]Department of Translational and Precision Medicine, University La Sapienza, Rome, Italy.

[9]Department of Cell and Developmental Biology, Perelman School of Medicine, University of Pennsylvania, Philadelphia, PA 19104, USA.

*mpack@pennmedicine.upenn.edu

Abstract

Extra-hepatic biliary atresia (BA) is an important pediatric liver disease of unknown etiology. The identification of biliatresone, a plant electrophile with selective toxicity for extra-hepatic cholangiocytes (EHC) and linked to outbreaks of epidemic BA in livestock, demonstrated the feasibility of an environmental trigger for this enigmatic condition. Here, we show that susceptibility of zebrafish EHC to biliatresone arises from their inability to restore stress-induced depletion of glutathione, and that heterozygous mutations in glutathione metabolism genes differentially sensitize EHC and the normally resistant intra-hepatic cholangiocytes (IHC) to biliatresone-mediated injury. Collectively these findings argue that genetic variants in stress-response genes could be risk factors for human BA. Supporting this idea, we identified *de novo* loss-of-function mutations in the *STIP1* and *REV1* gene, both part of the HSP90 pathway, in two children with BA, respectively, and showed that modulation of their expression sensitized zebrafish larvae and human cholangiocytes to biliatresone. Using an *in vivo* drug screening assay, we identified activators of cGMP signaling as potent enhancers of the anti-oxidant *N*-acetylcysteine (NAC) in biliatresone-treated larvae and human cholangiocytes that act independently of glutathione and upstream of chaperone-mediated protein quality control (PQC) pathways. Collectively, these data highlighted novel aspects of cholangiocyte injury responses, identified new genetic risk factors for BA, and suggest combined treatment with NAC and cGMP signaling modulators as a rational therapeutic strategy for BA.

Introduction

Extra-hepatic biliary atresia (BA) is a fibrosing cholangiopathy of infancy that is the most common indication for pediatric liver transplantation (*1-4*). The etiology of BA has long been debated (*4*). A minority of BA cases occurs as part of multi-organ developmental syndromes, thus supporting a genetic etiology; however, genetic factors have not been conclusively identified for the majority of cases, which occur in the absence of other defects (referred to as isolated BA). The most commonly accepted mechanistic model posits that BA is a complex disease resulting from exposure of genetically susceptible individuals to an environmental trigger, such as a toxin or virus, during late gestation (*5-8*). In this model, exposure to commonly encountered agents would trigger BA in individuals with rare genetic variants, and conversely, rare exposures might trigger BA in individuals with common variants.

Using a zebrafish bioassay, we isolated the electrophilic isoflavone biliatresone, from *Dysphania* species plants, whose maternal ingestion has been linked to epidemic BA in newborn livestock (*9*). Biliatresone is the first environmental agent linked to a naturally occurring BA phenotype. Initial biochemical analyses suggested that the biliatresone alpha-methylene Michael acceptor, which is capable of forming adducts with reduced glutathione (GSH), nucleic acids and amino acids, was important for its toxicity (*10, 11*). This was subsequently confirmed with structure activity relationship studies using zebrafish larvae and mammalian cholangiocyte spheroids (*12*). Additional studies in the zebrafish model showed that the selective toxicity of biliatresone toward EHC correlated with intracellular glutathione redox potential, and that genetic disruption of *nuclear factor, erythroid 2-like* (*nrf2*), a key transcriptional regulator of anti-oxidant defenses (*13*), broadened biliatresone's toxicity profile, leading to destruction of the normally resistant

intrahepatic cholangiocytes (IHC). These findings identified biliatresone as a potent cellular oxidant. Supporting this injury model, treatment of larvae with the anti-oxidant N-acetylcysteine (NAC), a synthetic precursor of GSH, significantly delayed the onset of biliatresone toxicity (*14*).

Although a causative role for an electrophilic toxicants in human BA is unproven, redox-mediated injury has been implicated in BA and two other human cholangiopathies, primary biliary cholangitis and primary sclerosing cholangitis (*15-19*). The inciting injury in these conditions has not been determined, and likely differs from one another, however the disruption of defense mechanisms that allow cholangiocytes to withstand the oxidizing effect of continuous bile exposure is considered to be a common contributory factor. Hydrophobic bile acids in human bile have well characterized disruptive effects on mitochondrial function and proteostasis (*20-24*), and we speculate that stress-induced injury from bile acids can potentiate injury from environmental exposure to biliatresone or related agents. Implicit in this model is the idea that genetic variants that modify cellular stress responses can be BA risk factors.

To gain a better understanding of the mechanisms underlying cholangiocyte sensitivity to redox and proteomic stress, we examined how genetic manipulation of glutathione metabolism and heat shock chaperone-mediated protein quality control (PQC) affected biliatresone toxicity in zebrafish larvae and human cholangiocytes. Leveraging the screening capabilities of the zebrafish system, we identified pharmacological activators of cGMP signaling as protective of biliatresone-mediated injury, independent of glutathione metabolism but dependent on the Hsp70/Hsp90 chaperone system. Linking these findings to human BA, we report here *de novo* genetic variants in the *STIP1* gene, which encodes the Hsp70-Hsp90 organizing protein (HOP), and *REV1*, which codes for a

HSP90 client protein involved in replication stress (*25*), (*26*), in two children with isolated BA. Collectively, the findings from this study suggest novel approaches to identify and treat children at risk for BA and other cholangiopathies.

Results

Genetic disruption of Glutathione metabolism genes in zebrafish

To gain insight into the differential sensitivity of zebrafish cholangiocytes to electrophilic stress, we analyzed the effect of biliatresone in larvae carrying loss-of-function mutations in glutathione metabolism genes. To study the role of glutathione synthesis and transport, we used CRISPR-Cas9 genome editing to disrupt *gclm*, which encodes the regulatory subunit of the rate-limiting enzyme in GSH synthesis, glutamate cysteine ligase (Gcl) (*27*), and *abcc2* (*28*), which encodes the canalicular transporter, Mrp2, that is required for GSH secretion from hepatocytes into bile. Mrp2 plays a central role in biliary GSH metabolism, as cholangiocytes synthesize GSH by degrading and resynthesizing GSH present in bile. Compared to the *gclm* mutation, which disrupts GSH synthesis in all cell types, mutation of *abcc2* specifically alters GSH synthesis in cholangiocytes. To study the role of GSH regeneration from its oxidized form GSSG (*27*), we analyzed larvae carrying a previously uncharacterized nonsense mutation in the *glutathione reductase* (*gsr*) gene (sa15125) that was generated *via* chemical mutagenesis (Fig. 1A, Table. S1).

Larvae homozygous for each mutation developed normally with normal hepatobiliary function and structure (Fig. 1B-D). Adult mutants had normal fertility and lifespan with the locations of the nonsense mutations in all three genes (confirmed *via* genomic and cDNA sequencing) predicting either complete or significant loss of function (Fig. 1A). Supporting this, quantitative RT-PCR

showed significantly reduced levels of each targeted transcript, presumably as a result of nonsense-mediated mRNA decay (Fig. 1E). Mass spectrometry studies also confirmed that each mutation had the predicted effect on GSH levels, namely a pronounced reduction in the total hepatic GSH content of *gclm* mutants compared to their WT siblings, as well as a significant decrease in bile GSH measured in gallbladders dissected from adult *abcc2* mutants (Fig. 1F, G). Total hepatic GSH was not affected in *gsr* larvae, similar to *Gsr* mice (*29*) (Fig. 1F).

Mutations of glutathione metabolism genes alter cellular redox status

To determine how mutations in glutathione metabolism genes affect the basal glutathione redox state of different liver cell types, we crossed the mutant lines into transgenic fish carrying a ubiquitously expressed cytoplasmic redox biosensor Grx-roGFP2 (hereafter, roGFP)[1,29]. This highly sensitive and specific *in vivo* probe contains an engineered dithiol/disulfide switch that provides a ratiometric readout of fluorescence emission at two excitation wavelengths (405 and 488 nm). A high 405nm:488nm excitation ratio indicates an oxidized sensor (low GSH:GSSG ratio), whereas a low ratio signifies a reduced state (high GSH:GSSG ratio).

Previous work showed that EHC of wild type zebrafish larvae are oxidized compared to IHC and hepatocytes, and that short duration exposure of larvae to biliatresone (4 hr) causes further oxidation of EHC, thus predicting overt injury that is first evident at 16-24 hr post-treatment (*14*). Based on these earlier findings, we hypothesized that the effects of the glutathione metabolism gene mutations on basal glutathione redox status would provide insight into cellular sensitivities to oxidative stress, such as with exposure to biliatresone.

We first analyzed homozygous *gclm* mutants, whose dysfunctional GSH synthesis machinery, was predicted to oxidize the glutathione pool of EHC, IHC and hepatocytes. The roGFP measurements confirmed this prediction in the homozygotes, with normal hepatic redox heterogeneity observed in the wild type (WT) and heterozygous sibling larvae (Fig. 1H, I). Next, we analyzed *gsr* mutants. Basal redox potential was also oxidized in all three liver cell types of homozygous mutants, most likely secondary to increased GSSG (Fig. 1J, K). However, oxidation was less than in *gclm* homozygotes, possibly reflecting a compensatory increase in GSH synthesis in Gsr deficient cells. Redox status was not altered in *gsr* heterozygotes (Fig. 1J, K). The *abcc2* mutation, which was predicted to have different effects on cholangiocytes and hepatocytes, was analyzed last. Homozygous *abcc2* mutation oxidized the glutathione pool of EHC and IHC, consistent with reduced GSH transport into bile, but had no effect on hepatocytes (Fig. 1F, L, M). Heterozygous mutation of *abcc2* oxidized the glutathione pool of EHC but not IHC, suggesting reduced GSH synthetic capacity in EHC compared to IHC (Fig. 1L, M).

Changes in redox status imparted by mutations in glutathione metabolism genes reveal cell-type specific responses to electrophilic stress

Having defined the effects of glutathione metabolism gene mutations on basal redox status, we next asked whether they were predictive of sensitization to biliatresone in either EHC or IHC. For this study, we define sensitization as EHC injury caused by a normally inactive low dose of the toxin (0.25 µg/ml; Fig. A, B), or IHC injury caused by either the low dose, or the standard dose (0.5 µg/ml), which only induces EHC injury in WT larvae (Fig. 2A, C).

Previous studies of biliatresone in the zebrafish model suggested that oxidizing mutations would

sensitize cholangiocytes to biliatresone (*14*). Consistent with these predictions, we observed that the oxidized EHC of *gclm*, *abcc2* and *gsr* mutants were all sensitized to low dose biliatresone (Fig. 2D, E, F, J, L). The oxidized IHC of *gclm* homozygotes and *abcc2* homozygotes were sensitized to low and standard doses of the toxin, respectively (Fig. 2D, H, M). Interestingly, basal redox status was not always predictive of biliatresone sensitization. Specifically, we observed sensitization of IHC in *abcc2* heterozygotes and EHC in *gsr* heterozygotes, even though the basal redox potential was not significantly different from their WT siblings (Fig. 2G, I, L, M). Conversely, the IHC of *gsr* homozygotes were resistant (not sensitized) to biliatresone despite their oxidation (Fig. 2K).

Collectively, these findings identify important differences in the way EHC and IHC maintain redox homeostasis in response to oxidative stress. EHC, as evidenced by their sensitization in *gclm*, *abcc2*, and *gsr* mutants, rely on both GSH synthesis and GSH regeneration. In contrast, IHC rely only on GSH synthesis, as demonstrated by their resistance to biliatresone even when oxidized in regeneration-deficient *gsr* homozygotes. The importance of GSH synthesis in IHC is further underscored by their sensitization in non-oxidized *abcc2* heterozygotes.

Biliatresone induces proteomic stress and modulation of the Hsp90 chaperone machinery enhances biliatresone toxicity

Prior hepatic expression profiling experiments showed that in addition to glutathione metabolism genes, genes involved in the maintenance of cellular proteostasis were upregulated in the initial response to biliatresone (*14*). Quantification of polysomal mRNA isolated from larval biliary cells (EHC & IHC) and hepatocytes *via* translating ribosomal affinity profiling (TRAP) methodology

(*30*) confirmed the induction of heat shock response (HSR) and unfolded protein response/endoplasmic reticulum (UPR/ER) stress response genes in both cell types 4 hr after biliatresone exposure (Fig. 3A). To test the functional significance of these findings, we asked whether WT larvae treated with the heat shock protein 90 (Hsp90) inhibitor 17-*N*-allylamino-17-demethoxygeldanamycin (17-AAG) (*31, 32*) were sensitized to low-dose biliatresone. Conversely, we also examined whether pre-treatment with geranylgeranyl acetate (*33*), an activator of heat shock protein 70 (Hsp70) (*33, 34*), which functions upstream of Hsp90 during the folding of newly synthesized and denatured proteins, could blunt biliatresone-mediated injury. We found that inhibition of Hsp90 sensitized EHC to low-dose biliatresone (Fig. 3B-F, J), whereas pre-treatment with the Hsp70 activator did not mitigate its toxic effect (Fig. 3H-J). Significantly, the GSH synthetic precursor NAC was unable to attenuate the sensitization caused by Hsp90 inhibition (Fig. 3G, J). Altogether, these data suggest that the Hsp70/Hsp90 chaperone machinery plays a crucial role in the cellular response to biliatresone that is independent of the glutathione-mediated redox response.

Activation of cGMP signaling rescues biliatresone-mediated cholangiocyte injury in zebrafish and human cholangiocytes

The discovery that biliatresone affected protein quality control independently of redox homeostasis indicated that it might be possible to enhance the protective effect of NAC by activating other stress response pathways. To test this idea, we screened a library of known drugs (JHCC; Version 1.0) for their ability to blunt EHC damage in biliatresone-treated larvae. Of 1514 drugs screened, a consistent effect was only seen with two drugs, the phosphodiesterase inhibitors (PDEi) aminophylline and trequinsin. Aminophylline is a non-specific PDEi that blocks the

hydrolysis of cAMP and cGMP in a broad range of cell types (*35*). Trequinsin preferentially targets PDE isoform 3 (PDE3), also leading to increased levels of cAMP and cGMP (*36, 37*). To confirm the specificity of these results, we co-treated larvae with standard dose biliatresone and independently sourced PDEi for 72 hr (Table S3). These experiments confirmed the activity of aminophylline, with 56.0% of treated larvae exhibiting normal or minimally injured EHC (Fig. 4D, J), in contrast to 95% of larvae exhibiting severe EHC abnormalities that were treated biliatresone alone (Fig. 4B). The response to trequinsin, on the other hand, was inconsistent (data not shown). Interestingly, two PDE5 inhibitors, vardenafil (Levitra) and tadalafil (Cialis), which block cGMP degradation and are clinically approved for erectile dysfunction and pulmonary hypertension (*38, 39*), had a comparable effect as aminophylline in 60.0% and 49.5% of the larvae examined, respectively (Fig. 4E, J, S1D, J).

To confirm that PDEi-mediated rescue arose from activation of cGMP signaling, we examined the effect of the cGMP analog 8-Bromoguanosine 3',5'-cyclic monophosphate (8-Br-cGMP)[36], and the heme-dependent and independent activators of soluble guanylate cyclase (sGC) (BAY 41-2272 and BAY 58-2667) in biliatresone-treated larvae. All three treatments imparted resistance to biliatresone that was comparable to treatments with the PDEi (Fig. 4F, J; Fig.S1E, F, J). In contrast, co-treatment with the adenylate cyclase activator, forskolin[39], which increases levels of cAMP, but not cGMP, did not reduce biliatresone-toxicity (Fig. S2)

Activation of cGMP signaling had a comparable effect on biliatresone toxicity in two human cholangiocyte cell lines (H69 and NHC) (*40, 41*). On its own, standard dose biliatresone (1.0 μg/ml) disrupted microtubules, as evidenced by reduced immunostaining for acetylated tubulin,

which was previously shown in biliatresone-treated mouse cholangiocytes (*9, 42*), and by decreased cell survival in both cell lines (Fig. 5A, B, J, S3A, B, J). Both toxicity readouts were significantly reduced by treatment with PDEi and 8-Br-cGMP (Fig. 5D-F, J, S3D-F, J). Interestingly, cGMP levels were not reduced by biliatresone (Fig. S4), suggesting that endogenous cGMP signaling may not be affected by biliatresone. These findings confirm that activation of cGMP signaling can rescue biliatresone-mediated injury in both zebrafish and human cholangiocytes.

cGMP signaling functions independently of glutathione anti-oxidant responses

To examine the relationship of cGMP signaling to glutathione-mediated injury responses, we asked whether PDE5 inhibitors or 8-Br-cGMP enhanced the ability of NAC to delay EHC injury in biliatresone-treated zebrafish larvae. We found that activation of cGMP signaling in zebrafish significantly improved the effect of NAC, with 80-90% of larvae showing normal EHC or minimal EHC injury after 72 hr of treatment with standard dose biliatresone (Fig. 4G-J, S1G-J). NAC monotherapy, on the other hand, had no effect on biliatresone toxicity at this treatment time point (Fig. 4C, J, S1C, J). Highly comparable effects were also observed in co-treatment of the human cholangiocyte cell lines exposed to biliatresone (Fig. 5C, G-J, S3C, G-J).

As further proof that cGMP signaling functioned independently of glutathione-mediated responses, we examined the effect of vardenafil and 8-Br-cGMP in biliatresone-treated *gclm* mutants and observed mitigation of EHC injury in 62.5% and 70.8% of mutant larvae (Fig. S5A-E). Importantly, they did so without altering total hepatic GSH levels, which were reduced comparably in the mutants regardless of whether they received vardenafil or 8-Br-cGMP (Fig.

S5F).

Exome sequencing identifies deleterious rare variants in the stress-induced Hsp90 co-chaperone STIP1 and in a child with BA

As part of an independent study, we carried out exome sequencing in 30 probands with isolated BA ascertained through the NIDDK-funded Childhood Liver Disease Research Network (*43*) and their parents, to identify potentially causal *de novo* variants. Complete results of this large-scale exome sequencing project will be reported elsewhere. In one individual, we identified a *de novo* heterozygous stop-gain variant (NP_001269581:p.(Cys30Ter)) in a primate-specific isoform of the stress-inducible HSP90 co-chaperone *STIP1* (isoform 1) (Fig. 6A, B, S6). STIP1 is an evolutionarily conserved protein whose interactions with HSP70 and HSP90 orthologs have been demonstrated in yeast and rodents (*44-46*). The BA-associated *STIP1* variant targets the longest transcript isoform, which possesses an additional 47 amino acids at the N- terminus compared to other protein isoforms. This variant was detected in the BA patient, but not present in either parent (familial relationships confirmed with exome data), and is found with a minor allele frequency of 0.002% (3 heterozygous alleles) in the population variant database gnomAD. In a second individual, we identified a novel obligatory splice-site mutation in intron 10-exon 11 boundary of the gene *REV1* that affects all isoforms. *REV1* encodes a Y-family polymerase that plays a central role in translesion DNA synthesis during replication stress and has been shown to be a HSP90 client protein (*25, 26*).

To test the hypothesis that nonsense variant in *Stip1* or *Rev1* could exacerbate biliatresone-mediated injury, we first used CRISPR-Cas9 to engineer loss-of-function mutations in the

zebrafish orthologs of these genes. The resulting frameshift mutations were confirmed *via* cDNA sequencing (Fig. 6C). Interestingly, whereas STIP1 knockout mice are embryonically lethal due to placental disruption, zebrafish deficient in Stip1 develop normally. Although these mutant fish can survive to adulthood under unstressed conditions, their ability to respond to toxic insults is compromised, including in heterozygous carriers. Specifically, we observed pronounced EHC injury in 75.0% heterozygous and 86.3% homozygous mutant larvae exposed to low-dose biliatresone (Fig. 6D-H, L). Complementary observation of impaired stress tolerance was also made in the *rev1* mutant fish with 66.67% of heterozygotes and 90% of homozygote showing severe EHC abnormality after low-dose toxin treatment (Fig. 6I-L).

To get a better understanding of the potential role of the *STIP1* isoform 1 mutation in human BA, we examined its expression in biliatresone-treated H69 cells. Interestingly, we found that while isoform-1 is not the predominant isoform in this cell type, its mRNA was up-regulated by 3.5 fold after 6 hr biliatresone exposure, whereas total *STIP1* mRNA was only increased 1.5 fold. –To determine if isoform-1 affects cholangiocyte responses to biliatresone, we asked whether its selective knockdown, *via* siRNA, sensitized H69 cells to a low dose of the toxin by examining for evidences of impaired stress tolerance as well as decreased viability. RT-PCR showed significant reduction in *STIP1-iso1* mRNA levels (70.6%) with no significant effect on total *STIP1* mRNA levels (Fig. 6M). This specific knockdown caused a pronounced destabilization of microtubules in cells treated with low-dose biliatresone along with decreased cell survival, whereas no severe tubulin depolymerization or changes in cell viability was seen with the control siRNA (Fig. 6O-R, W). Similar sensitization to biliatresone was observed with siRNA that target all *STIP1* isoforms, which led to significant reduction in both isoform-1 mRNA (82.6%) and *STIP1* total mRNA

(79.5%) (Fig. 6M, S, T, W). Western blot analyses showed that the non-selective siRNAs significantly reduced STIP protein (49.9%) whereas the isoform-1 siRNAs had no effect, either because the antibody doesn't recognize isoform-1, or because the endogenous protein level of this isoform is low relative to the non-targeted isoforms (Fig. 6N).

Since STIP1 has been shown to promote DNA damage response (DDR) (*47, 48*), we also assessed for formation of nuclear foci of phosphorylated H2AX (γ-H2AX), which accumulate at sites of stalled replication forks and are a sensitive indicator of both DNA damage and replication stress. Interestingly, knockdown of total STIP1 protein led to induction of γ-H2AX foci in H69 cells treated with low-dose biliatresone, whereas no change in γ-H2AX phosphorylation was observed with isoform-1 specific STIP1 knockdown (Fig. 6O-T). Collectively, these data suggest that while STIP1 isoform-1 may play an important role in preventing cytoskeletal collapse mediated by exogenous electrophiles such as biliatresone, the other isoforms are essential for combatting oxidant-induced DNA damage.

Similar experiments were conducted in human cholangiocytes to examine the effect of REV1 depletion on biliatresone sensitivity. Treatment of H69 with REV1-specific siRNA resulted in significant REV1 knockdown, at both the mRNA and protein level (Fig. 6M,N). Although no apparent abnormality was observed in cells depleted of REV1 under unstressed conditions, pronounced accumulation of γ-H2AX associated with increased cell death was observed in cells exposed to low-dose biliatresone (Fig. 6U-W). Of note, REV1 knockdown did not lead to any apparent microtubule instability in cells treated with low-dose biliatresone, thus demonstrating a different injury mechanism than arises with STIP1 knockdown.

cGMP signaling functions upstream of the stress-induced heat shock response in biliatresone-treated zebrafish and human cholangiocytes

cGMP signaling has been shown to enhance proteasome-mediated degradation of misfolded proteins in cardiomyocytes (*49*). To determine whether cGMP functioned comparably in human cholangiocytes we first asked whether 8-Br-cGMP or PDE5i reversed upregulation of *HSP70* in biliatresone treated H69 cells. RT-PCR showed that this was the case, with near normalization of expression when both treatments were combined with NAC (Fig. 7A). To address this question with greater specificity in an *in vivo* setting, we asked if 8-Br-cGMP could ameliorate biliatresone toxicity in larvae with genetically or pharmacologically altered Hsp90/Hsp70 chaperone machinery. While we found that exogenous cGMP administration via 8-Br-cGMP could reverse sensitization of *stip1* heterozygotes to biliatresone, the treatment failed to rescue biliatresone toxicity in zebrafish larvae co-exposed to the Hsp90 inhibitor 17-AAG, thus arguing that cGMP activity requires an intact Hsp90 in zebrafish. (Fig. 7B-H, J).

While functional Stip1 is not required for cGMP-mediated amelioration of cholangiocyte injury in zebrafish, modulation of this co-chaperone does impact the protective effect exerted by cGMP in biliatresone-treated human cholangiocytes. Specifically, we found that 8-Br-cGMP was able to mitigate biliatresone-induced disruption of acetylated tubulin in cells transfected with isoform-1 specific siRNAs, but not in cells with total STIP1 knockdown, arguing that cGMP in human cholangiocytes is sensitive to levels of STIP1 protein and/or a unique function of isoform-1 (Fig. 7K-R).

Although cGMP activity may be dependent on an intact HSP90/70 chaperone machinery, it does not appear to rely on the HSP90 interacting protein REV1. Namely, we found that exogenous cGMP administration was able to attenuate EHD injury in *rev1* homozygous mutant sand reverse γ-H2AX accumulation in biliatresone-treated REV1-depleted cells (Fig. 7I, J, S,T).

Short exposure to biliatresone leads to progressive EHD damage in zebrafish larvae, which can be halted by enhancing redox homeostasis and cGMP signaling

As an environmental trigger for human BA has not been conclusively demonstrated, the timing and duration of exposure remain speculative. The recent observation that a rising total bilirubin level had high sensitivity and specificity for BA in newborn infants (*50*) suggests a prenatal exposure, presumably transient, can trigger progressive and irreversible biliary damage. Supporting this model of biliary injury, we found that short exposure to standard dose biliatresone (6 hr) induced minimal or no EHC injury at the end of the exposure period, consistent with prior studies (*14*), however the injury progressed in 64.3% of larvae by 24 hr post-treatment despite toxin removal (Fig. 8A-D, J). This suggests that once initiated, the damaging cascade amplifies and self perpetuates. We were able to halt this progression of injury by initiating combined treatment with the NAC & cGMP at the time of toxin removal, but not with NAC alone (Fig. 8E, J). We found that 78.9%-92.5% of larvae exposed to cGMP enhancers or the combination therapy exhibited normal EHC or minor epithelial damage compared with 35.7% of untreated larvae (Fig. 8D, F-J).

Discussion

There is a significant need for new treatments for BA, which despite being a rare condition is the most common indication for liver transplantation in the pediatric population. Unfortunately,

neither the inciting disease trigger, which leads to fibrotic destruction of the extra-hepatic biliary system, nor the cause of progressive intra-hepatic bile duct disease and subsequent liver failure has been determined. A perinatal viral illness has been the leading hypothesis for many years, however no viral culprit has been conclusively implicated in the human disease (*51, 52*).

The identification of biliatresone from *Dysphania* species plants was a significant advance for the field because it was the first conclusive evidence of a non-infectious environmental agent capable of causing BA (*9*). And while direct consumption of biliatresone by humans is unlikely, the toxin-induced BA model has provided novel insights into cholangiocyte injury mechanisms, and through this, insights into genetic risk factors and new treatment strategies, complementing ideas that have emerged from other BA models, particularly the mouse rotavirus infection model (*33, 53*).

The work reported here builds on previous studies in zebrafish that identified cholangiocyte redox reserve as an important factor in the selective toxicity of biliatresone to EHC (*14, 42*). Through *in vivo* measurement of redox potentials in glutathione metabolism gene mutants, we now show that EHC, with their low basal redox reserve, require both GSH regeneration and *de novo* GSH synthesis to combat oxidative stress. IHC, on the other hand, can tolerate a basal oxidized redox state associated with lack of GSH regeneration and remain poised to mitigate an exogenous oxidative insult. This most likely derives from their greater GSH synthetic capacity,
as even a modest reduction as occurs in *abcc2* heterozygotes with normal basal redox status, sensitizes to biliatresone. Sensitization of *abcc2* and *gsr* heterozygotes to biliatresone despite each mutant exhibiting normal basal redox potential highlights the possibility that redox gene variants could be otherwise silent risk factors for environmentally induced BA in humans.

The mechanism that accounts for differences in cholangiocyte GSH metabolism is unknown, however we hypothesize that it reflects the shared lineage of IHC and hepatocytes, which derive from a common progenitor (*54*). Hepatocytes have an extraordinarily high synthetic capacity for GSH compared to other cell types (*27*), and this is likely to be epigenetically regulated, at least in part. From this, we speculate that in IHC, the chromatin landscape surrounding genes needed for GSH synthesis may provide an advantageous response to environmental and/or endogenous stressors. Notably, risk imparted by modulation of the epigenetic factors could be additive to genetic variants in GSH metabolism genes, which on their own impart a small heritable disease risk that is not easily detected by predictive algorithms of protein function. Supporting this model, in prior work we demonstrated DNA hypomethylation in IHC relative to hepatocytes in BA infants at either the time of diagnosis or surgical repair, but not in infants with other cholestatic liver diseases, or in non-liver disease controls (*55*).

The limited GSH synthetic capacity of EHC revealed by the genetic analyses reported here is consistent with previous work showing that the onset of biliatresone toxicity is delayed by treatment with the GSH precursor, NAC. Interestingly, NAC administration has recently been shown to reduce liver injury and biliary fibrosis and increased survival times in the rotavirus-BA mouse model Furthermore, transplant-free survival of BA infants following Kasai portoenterostomy was also shown to be linked to elevated hepatic expression of GSH metabolism genes (*56*). Benefits afforded by NAC in the rotavirus model reflect reduced injury to IHC, which is consistent with increased susceptibility of zebrafish IHC to biliatresone when GSH synthesis is impaired (Fig. 2) (*14*). In human BA the effects of enhanced antioxidant capacity can have a variety

of effects that impact clinical outcomes, however it is plausible that reduced severity of biliary fibrosis, arising from mitigating IHC injury, plays a contributory role. Collectively, these data suggest that redox metabolism may play a crucial role in driving BA pathogenesis regarding of the inciting event.

While NAC does provide protection against biliatresone, its effect is transient, likely because the toxin activates additional stress response pathways either in parallel or downstream of glutathione-mediated responses. Supporting this idea, transcriptional profiling showed pronounced activation of the heat shock chaperone system, which when disrupted pharmacologically, with the pan-Hsp90 inhibitor 17-AAG, or genetically, *via* mutating the co-chaperone *stip1* or HSP90 client protein *rev1*, sensitized the larvae to the toxin. The observed sensitization was not mitigated by NAC, arguing that the proteostasis pathways are activated by biliatresone independently of the initial glutathione-mediated redox response.

Altered proteostasis has not been previously implicated in human BA, however a proteomic study found that hepatic levels of the inducible HSP90 isoform HSP90AA were reduced 20-fold in newly diagnosed BA infants compared to neonates with other cholestatic liver diseases (*58*). Assigning causality of this association is complicated by the fact that BA is typically diagnoses at an advanced stage. Our findings that the heat shock pathway is activated by biliatresone in the zebrafish larvae, coupled with sensitization imparted by siRNA knockdown and mutation of Stip1 and Rev1, which both interact with Hsp90, supports a causal role that the variants detected in these genes via exome sequencing are BA risk factors. The mechanism underlying this risk is uncertain. The *STIP1* variant is predicted to disrupt only the largest of the three translated transcripts. Although the

precise function of this primate-specific isoform has not been determined, it was rapidly and significantly upregulated upon exposure to biliatresone and its selective knockdown was sensitizing, thus arguing that this isoform plays an essential role in the cholangiocyte stress response. Tubulin immunostainings indicate that STIP1 isoform-1 maintains cytoskeletal integrity under conditions of oxidative stress, while the other isoforms are needed for the DNA damage response, as evidenced by accumulation of γ-H2AX foci, which are indicative of stalled replication or DNA damage. Collectively, these results demonstrate that in addition to maintaining proteostasis, both HSP90 and STIP1 also play crucial roles in maintaining cytoskeletal integrity and genome stability. These are consistent with prior studies showing their interactions with tubulin (*57-59*) and in regulating diverse DDR pathways *via* facilitating the folding of multiple DNA repair proteins, including p53 (*60*) and those involved in TLS such as REV1 (*26*).

Similar to our findings that *STIP1* and *REV1* haploinsufficiency lead to increased susceptibility to exogenous stressors such as biliatresone, mice and cells deficient in these genes also exhibit heightened sensitivity to certain stress-inducing conditions. For example, neurons of heterozygous *Stip1* knockout mice are highly sensitive to metabolic stress induced by cerebral ischemia (*47*), whereas cells deficient in Rev1 are defective in DDR as they are unable repair DNA interstrand crosslinks, which can be induced by chemical agents including electrophiles (*61*).

Although there is no prior reported association of *STIP1* or *REV1* polymorphisms with BA, our data strongly argue that while these rare loss of function variants are normally innocuous, under conditions of environmental or endogenous stress, they can predispose carriers to BA. One of the challenges in studying the genetic underpinnings of complex diseases lies is assigning causality to

variants of uncertain significance (*62*). Our results point to the power of using experimental models to identify pathogenic pathways, which can then be modulated to interrogate candidate genes, hence functionally connecting genetic variations with disease-relevant phenotypes.

The potential therapeutic role for cGMP signaling activators in BA is a novel finding to emerge from this study. cGMP signaling has been studied extensively in the context of cardiovascular disease as a mediator of nitric oxide-induced smooth muscle relaxation (*36*). Our observations indicate that the mitigating effect provided by cGMP to biliatresone-induced injury is mediated, at least in part, by the PQC machinery, either by enhancing protein refolding *via* the HSP70/HSP90 chaperone machinery or promoting proteasome degradation of denatured protein (*46*). cGMP activity depends on Hsp90 in the zebrafish larvae, however it does not appear to rely on the adapter protein Stip1 or the Hsp90 client protein Rev1. Specifically, cGMP did not impact biliatresone sensitization from Hsp90 inhibition but was able to confer protection in Stip1 and Rev1 knockout zebrafish. The role of STIP1 in mediating cGMP signaling appears more complicated in human cholangiocytes. cGMP prevented biliatresone-induced tubulin destabilization in H69 cells deficient in STIP1 isoform-1, but was unable to reverse the damage in cells with reduced levels of all STIP1 isoforms. The mechanism underlying this response is not known. cGMP level measurements argue that PDE5i and sGC stimulators do not simply restore cGMP levels altered by the toxin, but more likely modulate compartmentalized cGMP signaling, which has been observed in other cell types (*63, 64*).

Based on the additive ameliorative effects of combined NAC/cGMP in the biliatresone model we propose that combined use of these FDA-approved drugs can be used to prevent BA progression.

We envision two points of entry for the combination NAC/cGMP therapy in the timeline of BA. First, near the onset of extra-hepatic duct obstruction, which can be determined by measurement of conjugated bilirubin at birth and at 2-3 weeks of age, before the onset of symptoms (*50*). This approach has a high sensitivity and specificity for detecting BA, albeit with a low positive predictive value, in keeping with the rarity of the disease. Given the severity and progressive nature of BA, and that both NAC and PDE5 inhibitors are well tolerated in infants (*65-69*), combining treatments at this time point may be the most effective strategy, particularly if confirmatory studies can be performed allowing for treatment discontinuation in non-responders and those found not to have BA. Going forward, substitution of PDE5i with activators or stimulators of cGMP might be considered.

The second point of entry for treatment of BA infants with NAC/cGMP would be at the usual time of diagnosis, at 1 to 2 months of age (*50*). At this stage, there is irreversible damage to the extra-hepatic ductal system and varying degrees of portal fibrosis. Institution of NAC/cGMP therapy following the Kasai hepatoportoenterostomy (HPE), either on its own, or in combination with an immune modulator, has the potential to improve bile drainage post-HPE and reduce ongoing biliary injury that eventually culminates in biliary fibrosis. Administration of NAC/cGMP at this later stage has the benefit of preventing treatment of non-BA infants, albeit at the cost of treatment delay.

The cause of biliary fibrosis following restoration of bile flow post-HPE is unknown but presumably reflects persistent activation of cholangiocyte damage pathways triggered by the inciting injury, combined with bile acid-mediated injury and secondary activation of adaptive

immunity. Given that temporary exposure of zebrafish larvae to biliatresone led to progressive injury, we speculate that activation of damage pathways following a transient environmental exposure can be self-sustaining, and that restoring redox and proteostatic homeostasis will be critical in preventing further biliary injury, thereby halting disease progression.

Materials and Methods

Fish care and strains. The wild-type (WT) strains (TL, AB), transgenic strains (Tg (*ef1a*:Grx-roGFP; Tg(*Tp1*:mCherry), (*Tg(fabp10a:TRAP)*; (*Tg(krt18:TRAP)*) and mutant strains (*gclm*, *abcc2*, *gsr*, *stip1, rev1*) were used for the present studies. All zebrafish were raised in the University of Pennsylvania School of Medicine (Philadelphia, PA) zebrafish facility in accord with protocols approved by the University of Pennsylvania Institutional Animal Care and Use Committee.

Generation of targeted mutations in zebrafish using CRISPR/Cas9 system. The target sequences for *gclm, abcc2, stip1* were identified using the CHOPCHOP website: http://chopchop.cbu.uib.no/. The single-guide RNA (sgRNA) was generated as described(*70*). Cas9 protein were obtained from PNABIO. Approximately 60 to 120 pg of sgRNA and 180 pg of Cas9 protein were co-injected into WT embryos at the one-cell stage. Genomic DNAs was extracted from pools of 20 one-day old embryos, and the targeted areas were amplified and sequenced using primers listed in Supplementary Table 1 to confirm somatic mutations. Injected embryos were raised to adulthood (F0) and screened for the germline-transmitting founders. The F0 founders were subsequently outcrossed with WT fish to obtain the heterozygous F1 and F2 offspring. All experiments were performed on the animals of F3 or subsequent generations. The *gclm*, *abcc2* mutants were

genotyped using primers listed in Table S1. The *gsr* and *stip1* mutant fish were genotyped using the KASP genotyping assays (KBioscience).

Redox-Sensitive GFP Redox Mapping Double transgenic (*Tg(ef1a:Grx-roGFP; tp1:mCherry)*) larvae in *gclm, abcc2, gsr* genetic background were used for the redox mapping of hepatocytes, IHCs, and EHCs. *Tg(ef1a:Grx-roGFP)* is a redox biosensor line previously generated in our laboratory. Conservation of the biosensor redox state was achieved with the thiol-alkylating agent, N-ethylmaleimide (NEM), and the protocol was adapted from a previous study of deep tissue fluorescence redox imaging in adult Drosophila and was performed as previously described (*14, 71*).

GSH Derivatization and Liquid Chromatography/Mass Spectrometry. The GSH content was measured in larvae livers of as previously described(*14*). Five larval livers (including the extrahepatic biliary system) were used per sample.

Cell culture. H69 cells, an SV40-transformed (i.e. immortalized) normal human cholangiocyte cell line, and low passage number normal human cholangiocytes (NHCs) were obtained from Nicholas F. LaRusso (Mayo Clinic) and grown in H69 media as previously described (*72*).

Drug Treatments. Zebrafish larvae reared in 24-well plates were exposed to lyophilized biliatresone resuspended in anhydrous dimethyl sulfoxide (DMSO, 0.5% in embryo medium) for 24-72 hr. The larvae were either treated with low-dose biliatresone (0.25 μg/ml) or the standard dose (0.5 μg/ml) depending on the experimental condition. Additional compounds were used for the zebrafish studies at the indicated dose: N-acetylcysteine (NAC; Sigma-Aldrich; 20μM),

aminophylline (Selleckchem, 100μM), vardenafil (Selleckchem, 1.5μM), tadalafil (Selleckchem, 1.5μM), 8-Bromoguanosine 3',5'-cyclic monophosphate (8-Br-cGMP, Sigma-Aldrich, 25μM), BAY 41-2272 (Sigma-Aldrich, 50μM), BAY 58-2667 (Sigma-Aldrich, 10μM), forskolin (Sigma-Aldrich, 0.5μM); 17-*N*-allylamino-17-demethoxygeldanamycin (17-AAG, Sigma-Aldrich, 13.2μM); geranylgeranyl acetate (GGA, Sigma-Aldrich, 20μM). The medium containing each compound was changed daily. All assays were repeated three times with at least 30 treated larvae and an equal number of control larvae in the zebrafish experiments.

Cultured cholangiocytes were exposed to either low-dose biliatresone (0.50 μg/ml) or the standard dose (1.0 μg/ml) for 6-24 hr depending on the experimental condition. Additional compounds were used for the cell studies at the indicated dose: NAC (10μM), aminophylline (60μM), vardenafil (5μM), tadalafil (5μM), 8-Br-cGMP (500μM).

Immunofluorescence. After chemical treatments, larvae or cells were immunostained with mouse monoclonal antibody Annexin A4 (Abcam, Cambridge, MA), or acetylated tubulin (Sigma-Aldrich), respectively, and processed for confocal microscopy as previously described (*14*). Increased gain was applied to samples, if necessary, to visualize hypoplastic intrahepatic ducts in zebrafish larval liver.

Nanostring nCounter assay and data analysis. Actively translating mRNA was extracted from larval hepatocytes and cholangiocytes (*Tg(fabp10a:TRAP)*; (*Tg(krt18:TRAP)*) using the translating ribosomal affinity purification (TRAP) methodology as previously described (*14, 30*). n = 150-300 larvae dissected per condition. Gene expression analysis was performed with the

nCounter system (NanoString Technologies) as previously described (*14*). The input RNA was 100 ng per sample. The nCounter system uses molecular barcodes for direct digital detection of individual target mRNA molecules. The raw data were first normalized to the positive controls provided by the manufacturer, which accounted for variations in hybridization and purification efficiency, and then to three housekeeping genes (*bactin2*, *ef1a*, *rpl19*). The experiment was done in three biological replicates and differential gene expression was calculated relative to DMSO-treated controls.

siRNA Transfection. H69 cells were transfected with neg control siRNA (ON TARGET *plus* Non-targeting siRNA, Dharmacon), STIP1-iso1 siRNAs, STIP1-total siRNAs using DharmaFECT (Dharmacon) according to the manufacturer's protocol. Cells were subsequently treated with biliatresone (0.5 ug/ml) 24 hr post transfection for an additional 24 hr prior to further analyses. A 25 nM concentration of siRNA was used for all transfections.

RNA Extraction and qRT-PCR. RNA was isolated from zebrafish larval liver or cultured cholangiocytes using RNeasy Micro Kit (QIAGEN). RNA samples were quantified using a Nanodrop spectrophotometer (Thermo Fisher Scientific). Synthesis of cDNA from RNA samples was carried out using the SuperScript III First-Strand Synthesis System (Thermo Fisher Scientific). Real-time RT PCR was performed using Applied Biosystems StepOnePlus and SYBR green PCR Master Mix (Thermo Fisher Scientific) with primers listed in Table S2.

Protein Extracts and Western Blots. Cells were lysed in Lysis M buffer (Roche), and lysates were sonicated and pelleted. Supernatants were denatured and 30ug of protein was separated by poly-

acrylamide gel electrophoresis (Invitrogen), and then transferred to nitrocellulose membranes (Invitrogen). The following antibodies were used: STIP1 (Atlas Antibodies), REV1 (Santa Cruz, CA), β-actin (Santa Cruz, CA), and secondary anti-rabbit IgG (H+L)-HRP conjugate (Invitrogen) and anti-mouse IgG (H+L)-HRP conjugate (Invitrogen) antibodies. Enhanced chemiluminescence images were analyzed and quantified with ImageJ.

Cell Viability Assay. Cell viability assays were performed using tetrazolium compound based CellTiter 96® AQueous One Solution Cell Proliferation (MTS) assay (Promega). Biliatresone-treated H69 were co-exposed to PDEI with and without NAC. MTS assay was then performed according to the manufacturer's instruction at 48 hr post-treatments.

Exome Sequencing Analysis of Patients with Isolated Biliary Atresia. Patient samples: BA patient samples were obtained from the National Institute of Diabetes and Digestive and Kidney Diseases (NIDDK)-funded Childhood Liver Disease Research Network. Patients were enrolled into the ChiLDReN study at each participating site under IRB-approved protocols, and patients' data and blood samples had been obtained with informed consent from patients' parents or legal guardians. DNA samples from participants were isolated and banked at the Rutgers University NIDDK biorepository. De-identified DNA samples were sent to our laboratory for analysis. All patients were diagnosed with BA based on clinical presentation, liver histology, and intraoperative cholangiogram. The majority had their diagnosis confirmed by examination of the biliary remnant from HPE. A total of 30 patients with isolated BA and their parents (30 trios) underwent exome sequencing to identify potentially causal *de novo* variants. Complete results of this study will be reported elsewhere.

Exome sequencing analysis: Genomic DNA (3-5 ug) was supplied to Perkin Elmer, Inc. (Perkin-Elmer, Branford, CT) for whole exome sequencing of the BA patients and their parents. The DNA was amplified and enriched using the Agilent SureSelect V4+UTR 71Mb All Exon Capture Kit (Agilent Technologies, Santa Clara, CA). Sequencing was performed on the Illumina HiSeq 2000 (Illumina, San Diego, CA) at the Perkin-Elmer sequencing service center. All of the exome sequencing data was produced with paired-end reads of 100 bp in length (2 x 100bp). The unaligned FASTQ reads of all samples were returned for read analysis and downstream processing. Raw sequencing reads were mapped to GRCh37.69 reference genome using the Burrows-Wheeler Aligner (*6*) to produce an aligned BAM file. BAM files were realigned around known indels using IndelRealigner in GenomeAnalysisToolKit software (GATK) and base quality scores were recalibrated using BaseQualityScoreRecalibrator in GATK (*73*). Variant calling was performed using HaplotypeCaller (gVCF) and jointly genotyped using the GenotypeGVCFs command in GATK. The initial variant quality filtering was done using VariantQualityScoreRecalibrator (VQSR) in GATK. To identify potentially causal mutations, we filtered the identified variants for stop-gain, stop loss, frameshift and in-frame insertions/deletions, non-synonymous and splicing variants. SNPEff (*74*) was used to annotate the variants with functional consequence. We excluded variants overlapping with segmental duplications and variants with call rate less than 90%. We considered all variants present in a proband but absent in their parents as *de novo*, irrespective of their frequency in public databases. All the *de novo* variants were manually verified in the BAM file and a small subset, including the *STIP1* variant described here, was validated using Sanger sequencing.

Statistical Analyses. Data represent at least three independent experiments reported as means +/- SEM. The Student t test was used for comparison between two groups. Data from three or more groups were analyzed by one-way analysis of variance with Tukey's multiple comparisons test. $P < 0.05$ was considered to be significant.

References 1. B. A. Haber, P. Russo, Biliary atresia. *Gastroenterol Clin North Am* **32**, 891-911 (2003).

2. J. A. Bezerra, Potential etiologies of biliary atresia. *Pediatr Transplant* **9**, 646-651 (2005).

3. R. A. Schreiber, C. C. Barker, E. A. Roberts, S. R. Martin, F. Alvarez, L. Smith, J. D. Butzner, I. Wrobel, D. Mack, S. Moroz, M. Rashid, R. Persad, D. Levesque, H. Brill, G. Bruce, J. Critch, G. Canadian Pediatric Hepatology Research, Biliary atresia: the Canadian experience. *J Pediatr* **151**, 659-665, 665 e651 (2007).

4. C. L. Mack, A. G. Feldman, R. J. Sokol, Clues to the etiology of bile duct injury in biliary atresia. *Semin Liver Dis* **32**, 307-316 (2012).

5. E. A. Tsai, C. M. Grochowski, K. M. Loomes, K. Bessho, H. Hakonarson, J. A. Bezerra, P. A. Russo, B. A. Haber, N. B. Spinner, M. Devoto, Replication of a GWAS signal in a Caucasian population implicates ADD3 in susceptibility to biliary atresia. *Hum Genet* **133**, 235-243 (2014).

6. M. M. Garcia-Barcelo, M. Y. Yeung, X. P. Miao, C. S. Tang, G. Cheng, M. T. So, E. S. Ngan, V. C. Lui, Y. Chen, X. L. Liu, K. J. Hui, L. Li, W. H. Guo, X. B. Sun, J. F. Tou, K. W. Chan, X. Z. Wu, Y. Q. Song, D. Chan, K. Cheung, P. H. Chung, K. K. Wong, P. C. Sham, S. S. Cherny, P. K. Tam, Genome-wide association study identifies a susceptibility locus for biliary atresia on 10q24.2. *Hum Mol Genet* **19**, 2917-2925 (2010).

7. G. Cheng, C. S. Tang, E. H. Wong, W. W. Cheng, M. T. So, X. Miao, R. Zhang, L. Cui, X. Liu, E. S. Ngan, V. C. Lui, P. H. Chung, I. H. Chan, J. Liu, W. Zhong, H. Xia, J. Yu, X. Qiu, X. Z. Wu, B. Wang, X. Dong, J. Tou, L. Huang, B. Yi, H. Ren, E. K. Chan, K. Ye, P. F. O'Reilly, K. K. Wong, P. C. Sham, S. S. Cherny, P. K. Tam, M. M. Garcia-Barcelo, Common genetic variants regulating ADD3 gene expression alter biliary atresia risk. *J Hepatol* **59**, 1285-1291 (2013).

8. P. Harper, J. W. Plant, D. B. Unger, Congenital biliary atresia and jaundice in lambs and calves. *Aust Vet J* **67**, 18-22 (1990).

9. K. Lorent, W. Gong, K. A. Koo, O. Waisbourd-Zinman, S. Karjoo, X. Zhao, I. Sealy, R. N. Kettleborough, D. L. Stemple, P. A. Windsor, S. J. Whittaker, J. R. Porter, R. G. Wells, M. Pack, Identification of a plant isoflavonoid that causes biliary atresia. *Sci Transl Med* **7**, 286ra267 (2015).

10. K. W.-Z. Koo, O; Wells, R; Pack, M; Porter J, Reactivity of Biliatresone, a Natural Biliary Toxin, with Glutathione, Histamine and Amino Acids. *Chem Res Toxicol* **In Press** (2015).

11. K. A. Koo, K. Lorent, W. Gong, P. Windsor, S. J. Whittaker, M. Pack, R. G. Wells, J. R. Porter, Biliatresone, a Reactive Natural Toxin from Dysphania glomulifera and D. littoralis: Discovery of the Toxic Moiety 1,2-Diaryl-2-Propenone. *Chem Res Toxicol* **28**, 1519-1521 (2015).

12. M. A. Estrada, X. Zhao, K. Lorent, A. Kriegermeier, S. A. Nagao, S. Berritt, R. G. Wells, M. Pack, J. D. Winkler, Synthesis and Structure-Activity Relationship Study of Biliatresone, a Plant Isoflavonoid That Causes Biliary Atresia. *ACS Med Chem Lett* **9**, 61-64 (2018).

13. J. D. Hayes, A. T. Dinkova-Kostova, The Nrf2 regulatory network provides an interface between redox and intermediary metabolism. *Trends Biochem Sci* **39**, 199-218 (2014).

14. X. Zhao, K. Lorent, B. J. Wilkins, D. M. Marchione, K. Gillespie, O. Waisbourd-Zinman, J. So, K. A. Koo, D. Shin, J. R. Porter, R. G. Wells, I. Blair, M. Pack, Glutathione antioxidant pathway activity and reserve determine toxicity and specificity of the biliary toxin biliatresone in zebrafish. *Hepatology* **64**, 894-907 (2016).

15. I. Grattagliano, G. Calamita, T. Cocco, D. Q. Wang, P. Portincasa, Pathogenic role of oxidative and nitrosative stress in primary biliary cirrhosis. *World J Gastroenterol* **20**, 5746-5759 (2014).

16. L. N. Bell, J. Wulff, M. Comerford, R. Vuppalanchi, N. Chalasani, Serum metabolic signatures of primary biliary cirrhosis and primary sclerosing cholangitis. *Liver Int* **35**, 263-274 (2015).

17. D. R. Petersen, D. J. Orlicky, J. R. Roede, C. T. Shearn, Aberrant expression of redox regulatory proteins in patients with concomitant primary Sclerosing cholangitis/inflammatory bowel disease. *Exp Mol Pathol* **105**, 32-36 (2018).

18. U. Wasik, M. Milkiewicz, A. Kempinska-Podhorodecka, P. Milkiewicz, Protection against oxidative stress mediated by the Nrf2/Keap1 axis is impaired in Primary Biliary Cholangitis. *Sci Rep* **7**, 44769 (2017).

19. P. S. Leung, J. Choi, G. Yang, E. Woo, T. P. Kenny, M. E. Gershwin, A contemporary perspective on the molecular characteristics of mitochondrial autoantigens and diagnosis in primary biliary cholangitis. *Expert Rev Mol Diagn* **16**, 697-705 (2016).

20. T. Sousa, R. E. Castro, S. N. Pinto, A. Coutinho, S. D. Lucas, R. Moreira, C. M. Rodrigues, M. Prieto, F. Fernandes, Deoxycholic acid modulates cell death signaling through changes in mitochondrial membrane properties. *J Lipid Res* **56**, 2158-2171 (2015).

21. B. Yerushalmi, R. Dahl, M. W. Devereaux, E. Gumpricht, R. J. Sokol, Bile acid-induced rat hepatocyte apoptosis is inhibited by antioxidants and blockers of the mitochondrial permeability transition. *Hepatology* **33**, 616-626 (2001).

22. C. M. Payne, C. Crowley-Skillicorn, H. Holubec, K. Dvorak, C. Bernstein, M. P. Moyer, H. Garewal, H. Bernstein, Deoxycholate, an endogenous cytotoxin/genotoxin, induces the autophagic stress-survival pathway: implications for colon carcinogenesis. *J Toxicol* **2009**, 785907 (2009).

23. C. B. Ferrebee, J. Li, J. Haywood, K. Pachura, B. S. Robinson, B. H. Hinrichs, R. M. Jones, A. Rao, P. A. Dawson, Organic Solute Transporter alpha-beta Protects Ileal Enterocytes From Bile Acid-Induced Injury. *Cell Mol Gastroenterol Hepatol* **5**, 499-522 (2018).

24. M. Li, S. Y. Cai, J. L. Boyer, Mechanisms of bile acid mediated inflammation in the liver. *Mol Aspects Med* **56**, 45-53 (2017).

25. J. H. Yoon, J. Park, J. Conde, M. Wakamiya, L. Prakash, S. Prakash, Rev1 promotes replication through UV lesions in conjunction with DNA polymerases eta, iota, and kappa but not DNA polymerase zeta. *Genes Dev* **29**, 2588-2602 (2015).

26. F. M. Pozo, T. Oda, T. Sekimoto, Y. Murakumo, C. Masutani, F. Hanaoka, T. Yamashita, Molecular chaperone Hsp90 regulates REV1-mediated mutagenesis. *Mol Cell Biol* **31**, 3396-3409 (2011).

27. S. C. Lu, Glutathione synthesis. *Biochim Biophys Acta* **1830**, 3143-3153 (2013).

28. G. Jedlitschky, U. Hoffmann, H. K. Kroemer, Structure and function of the MRP2 (ABCC2) protein and its role in drug disposition. *Expert Opin Drug Metab Toxicol* **2**, 351-366 (2006).

29. J. Yan, X. Meng, L. M. Wancket, K. Lintner, L. D. Nelin, B. Chen, K. P. Francis, C. V. Smith, L. K. Rogers, Y. Liu, Glutathione reductase facilitates host defense by sustaining phagocytic oxidative burst and promoting the development of neutrophil extracellular traps. *J Immunol* **188**, 2316-2327 (2012).

30. B. J. Wilkins, W. Gong, M. Pack, A novel keratin18 promoter that drives reporter gene expression in the intrahepatic and extrahepatic biliary system allows isolation of cell-type specific transcripts from zebrafish liver. *Gene Expr Patterns* **14**, 62-68 (2014).

31. T. W. Schulte, L. M. Neckers, The benzoquinone ansamycin 17-allylamino-17-demethoxygeldanamycin binds to HSP90 and shares important biologic activities with geldanamycin. *Cancer Chemother Pharmacol* **42**, 273-279 (1998).

32. P. L. Yeyati, R. M. Bancewicz, J. Maule, V. van Heyningen, Hsp90 selectively modulates phenotype in vertebrate development. *PLoS Genet* **3**, e43 (2007).

33. K. Bessho, R. Mourya, P. Shivakumar, S. Walters, J. C. Magee, M. Rao, A. G. Jegga, J. A. Bezerra, Gene expression signature for biliary atresia and a role for interleukin-8 in pathogenesis of experimental disease. *Hepatology* **60**, 211-223 (2014).

34. S. Ikeyama, K. Kusumoto, H. Miyake, K. Rokutan, S. Tashiro, A non-toxic heat shock protein 70 inducer, geranylgeranylacetone, suppresses apoptosis of cultured rat hepatocytes caused by hydrogen peroxide and ethanol. *J Hepatol* **35**, 53-61 (2001).

35. D. M. Essayan, Cyclic nucleotide phosphodiesterases. *J Allergy Clin Immunol* **108**, 671-680 (2001).

36. G. Jedlitschky, B. Burchell, D. Keppler, The multidrug resistance protein 5 functions as an ATP-dependent export pump for cyclic nucleotides. *J Biol Chem* **275**, 30069-30074 (2000).

37. U. G. Friis, B. L. Jensen, S. Sethi, D. Andreasen, P. B. Hansen, O. Skott, Control of renin secretion from rat juxtaglomerular cells by cAMP-specific phosphodiesterases. *Circ Res* **90**, 996-1003 (2002).

38. R. C. Kukreja, F. N. Salloum, A. Das, Cyclic guanosine monophosphate signaling and phosphodiesterase-5 inhibitors in cardioprotection. *J Am Coll Cardiol* **59**, 1921-1927 (2012).

39. C. Unegbu, C. Noje, J. D. Coulson, J. B. Segal, L. Romer, Pulmonary Hypertension Therapy and a Systematic Review of Efficacy and Safety of PDE-5 Inhibitors. *Pediatrics* **139**, (2017).

40. J. M. Banales, E. Saez, M. Uriz, S. Sarvide, A. D. Urribarri, P. Splinter, P. S. Tietz Bogert, L. Bujanda, J. Prieto, J. F. Medina, N. F. LaRusso, Up-regulation of microRNA 506 leads to decreased Cl-/HCO3- anion exchanger 2 expression in biliary epithelium of patients with primary biliary cirrhosis. *Hepatology* **56**, 687-697 (2012).

41. S. A. Grubman, R. D. Perrone, D. W. Lee, S. L. Murray, L. C. Rogers, L. I. Wolkoff, A. E. Mulberg, V. Cherington, D. M. Jefferson, Regulation of intracellular pH by immortalized human intrahepatic biliary epithelial cell lines. *Am J Physiol* **266**, G1060-1070 (1994).

42. O. Waisbourd-Zinman, H. Koh, S. Tsai, P. Lavrut, C. Dang, X. Zhao, M. Pack, J. Cave, M. Hawes, K. Koo, J. R. Porter, R. G. Wells, Biliatresone, a toxin causing biliary atresia,

causes cholangiocyte disruption and fibrosis and acts through a pathway involving decreased GSH and Sox17. *Submitted*, (2015).

43. E. J. Thompson, K. Perez, C. P. Hornik, P. B. Smith, R. H. Clark, M. Laughon, C. Best Pharmaceuticals for Children Act-Pediatric Trials Network Steering, Sildenafil Exposure in the Neonatal Intensive Care Unit. *Am J Perinatol*, (2018).

44. A. Maciejewski, V. G. Ostapchenko, F. H. Beraldo, V. F. Prado, M. A. Prado, W. Y. Choy, Domains of STIP1 responsible for regulating PrPC-dependent amyloid-beta oligomer toxicity. *Biochem J* **473**, 2119-2130 (2016).

45. C. M. Nicolet, E. A. Craig, Isolation and characterization of STI1, a stress-inducible gene from Saccharomyces cerevisiae. *Mol Cell Biol* **9**, 3638-3646 (1989).

46. A. Rohl, D. Wengler, T. Madl, S. Lagleder, F. Tippel, M. Herrmann, J. Hendrix, K. Richter, G. Hack, A. B. Schmid, H. Kessler, D. C. Lamb, J. Buchner, Hsp90 regulates the dynamics of its cochaperone Sti1 and the transfer of Hsp70 between modules. *Nat Commun* **6**, 6655 (2015).

47. F. H. Beraldo, I. N. Soares, D. F. Goncalves, J. Fan, A. A. Thomas, T. G. Santos, A. H. Mohammad, M. Roffe, M. D. Calder, S. Nikolova, G. N. Hajj, A. L. Guimaraes, A. R. Massensini, I. Welch, D. H. Betts, R. Gros, M. Drangova, A. J. Watson, R. Bartha, V. F. Prado, V. R. Martins, M. A. Prado, Stress-inducible phosphoprotein 1 has unique cochaperone activity during development and regulates cellular response to ischemia via the prion protein. *FASEB J* **27**, 3594-3607 (2013).

48. J. A. Karam, R. Y. Parikh, D. Nayak, D. Rosenkranz, V. K. Gangaraju, Co-chaperone Hsp70/Hsp90-organizing protein (Hop) is required for transposon silencing and Piwi-interacting RNA (piRNA) biogenesis. *J Biol Chem* **292**, 6039-6046 (2017).

49. M. J. Ranek, E. J. Terpstra, J. Li, D. A. Kass, X. Wang, Protein kinase g positively regulates proteasome-mediated degradation of misfolded proteins. *Circulation* **128**, 365-376 (2013).

50. S. Harpavat, J. A. Garcia-Prats, B. L. Shneider, Newborn Bilirubin Screening for Biliary Atresia. *N Engl J Med* **375**, 605-606 (2016).

51. T. Saito, K. Shinozaki, T. Matsunaga, T. Ogawa, T. Etoh, T. Muramatsu, K. Kawamura, H. Yoshida, N. Ohnuma, H. Shirasawa, Lack of evidence for reovirus infection in tissues from patients with biliary atresia and congenital dilatation of the bile duct. *J Hepatol* **40**, 203-211 (2004).

52. S. Rauschenfels, M. Krassmann, A. N. Al-Masri, W. Verhagen, J. Leonhardt, J. F. Kuebler, C. Petersen, Incidence of hepatotropic viruses in biliary atresia. *Eur J Pediatr* **168**, 469-476 (2009).

53. M. Riepenhoff-Talty, K. Schaekel, H. F. Clark, W. Mueller, I. Uhnoo, T. Rossi, J. Fisher, P. L. Ogra, Group A rotaviruses produce extrahepatic biliary obstruction in orally inoculated newborn mice. *Pediatr Res* **33**, 394-399 (1993).

54. J. R. Spence, A. W. Lange, S. C. Lin, K. H. Kaestner, A. M. Lowy, I. Kim, J. A. Whitsett, J. M. Wells, Sox17 regulates organ lineage segregation of ventral foregut progenitor cells. *Dev Cell* **17**, 62-74 (2009).

55. R. P. Matthews, S. F. Eauclaire, M. Mugnier, K. Lorent, S. Cui, M. M. Ross, Z. Zhang, P. Russo, M. Pack, DNA hypomethylation causes bile duct defects in zebrafish and is a distinguishing feature of infantile biliary atresia. *Hepatology* **53**, 905-914 (2011).

56. Z. Luo, P. Shivakumar, R. Mourya, S. Gutta, J. A. Bezerra, Gene Expression Signatures Associated With Survival Times of Pediatric Patients With Biliary Atresia Identify Potential Therapeutic Agents. *Gastroenterology* **157**, 1138-1152 e1114 (2019).

57. Y. Wu, X. Zheng, Y. Ding, M. Zhou, Z. Wei, T. Liu, K. Liao, The molecular chaperone Hsp90alpha deficiency causes retinal degeneration by disrupting Golgi organization and vesicle transportation in photoreceptors. *J Mol Cell Biol*, (2019).

58. Y. Wu, Y. Ding, X. Zheng, K. Liao, The molecular chaperone Hsp90 maintains Golgi organization and vesicular trafficking by regulating microtubule stability. *J Mol Cell Biol*, (2019).

59. J. Li, X. Sun, Z. Wang, L. Chen, D. Li, J. Zhou, M. Liu, Regulation of vascular endothelial cell polarization and migration by Hsp70/Hsp90-organizing protein. *PLoS One* **7**, e36389 (2012).

60. V. Dahiya, G. Agam, J. Lawatscheck, D. A. Rutz, D. C. Lamb, J. Buchner, Coordinated Conformational Processing of the Tumor Suppressor Protein p53 by the Hsp70 and Hsp90 Chaperone Machineries. *Mol Cell* **74**, 816-830 e817 (2019).

61. C. Clauson, O. D. Scharer, L. Niedernhofer, Advances in understanding the complex mechanisms of DNA interstrand cross-link repair. *Cold Spring Harb Perspect Biol* **5**, a012732 (2013).

62. K. McAllister, L. E. Mechanic, C. Amos, H. Aschard, I. A. Blair, N. Chatterjee, D. Conti, W. J. Gauderman, L. Hsu, C. M. Hutter, M. M. Jankowska, J. Kerr, P. Kraft, S. B. Montgomery, B. Mukherjee, G. J. Papanicolaou, C. J. Patel, M. D. Ritchie, B. R. Ritz, D. C. Thomas, P. Wei, J. S. Witte, Current Challenges and New Opportunities for Gene-Environment Interaction Studies of Complex Diseases. *Am J Epidemiol* **186**, 753-761 (2017).

63. L. A. Piggott, K. A. Hassell, Z. Berkova, A. P. Morris, M. Silberbach, T. C. Rich, Natriuretic peptides and nitric oxide stimulate cGMP synthesis in different cellular compartments. *J Gen Physiol* **128**, 3-14 (2006).

64. R. K. Perera, J. U. Sprenger, J. H. Steinbrecher, D. Hubscher, S. E. Lehnart, M. Abesser, K. Schuh, A. El-Armouche, V. O. Nikolaev, Microdomain switch of cGMP-regulated phosphodiesterases leads to ANP-induced augmentation of beta-adrenoceptor-stimulated contractility in early cardiac hypertrophy. *Circ Res* **116**, 1304-1311 (2015).

65. H. E. Perry, M. W. Shannon, Efficacy of oral versus intravenous N-acetylcysteine in acetaminophen overdose: results of an open-label, clinical trial. *J Pediatr* **132**, 149-152 (1998).

66. R. H. Squires, A. Dhawan, E. Alonso, M. R. Narkewicz, B. L. Shneider, N. Rodriguez-Baez, D. D. Olio, S. Karpen, J. Bucuvalas, S. Lobritto, E. Rand, P. Rosenthal, S. Horslen, V. Ng, G. Subbarao, N. Kerkar, D. Rudnick, M. J. Lopez, K. Schwarz, R. Romero, S. Elisofon, E. Doo, P. R. Robuck, S. Lawlor, S. H. Belle, G. Pediatric Acute Liver Failure Study, Intravenous N-acetylcysteine in pediatric patients with nonacetaminophen acute liver failure: a placebo-controlled clinical trial. *Hepatology* **57**, 1542-1549 (2013).

67. A. Shiva, M. Shiran, M. Rafati, H. Zamani, K. Babazadeh, M. Saeedi, S. Ala, Oral Tadalafil in Children with Pulmonary Arterial Hypertension. *Drug Res (Stuttg)* **66**, 7-10 (2016).

68. M. R. Sabri, H. Bigdelian, M. Hosseinzadeh, A. Ahmadi, M. Ghaderian, M. Shoja, Comparison of the therapeutic effects and side effects of tadalafil and sildenafil after surgery in young infants with pulmonary arterial hypertension due to systemic-to-pulmonary shunts. *Cardiol Young* **27**, 1686-1693 (2017).

69. K. Tan, M. B. Krishnamurthy, J. L. O'Heney, E. Paul, A. Sehgal, Sildenafil therapy in bronchopulmonary dysplasia-associated pulmonary hypertension: a retrospective study of efficacy and safety. *Eur J Pediatr* **174**, 1109-1115 (2015).

70. J. A. Gagnon, E. Valen, S. B. Thyme, P. Huang, L. Akhmetova, A. Pauli, T. G. Montague, S. Zimmerman, C. Richter, A. F. Schier, Efficient mutagenesis by Cas9 protein-mediated oligonucleotide insertion and large-scale assessment of single-guide RNAs. *PLoS One* **9**, e98186 (2014).

71. C. Seiler, G. Davuluri, J. Abrams, F. J. Byfield, P. A. Janmey, M. Pack, Smooth muscle tension induces invasive remodeling of the zebrafish intestine. *PLoS Biol* **10**, e1001386 (2012).

72. J. H. Tabibian, C. E. Trussoni, S. P. O'Hara, P. L. Splinter, J. K. Heimbach, N. F. LaRusso, Characterization of cultured cholangiocytes isolated from livers of patients with primary sclerosing cholangitis. *Lab Invest* **94**, 1126-1133 (2014).

73. G. A. Van der Auwera, M. O. Carneiro, C. Hartl, R. Poplin, G. Del Angel, A. Levy-Moonshine, T. Jordan, K. Shakir, D. Roazen, J. Thibault, E. Banks, K. V. Garimella, D. Altshuler, S. Gabriel, M. A. DePristo, From FastQ data to high confidence variant calls: the Genome Analysis Toolkit best practices pipeline. *Current protocols in bioinformatics* **43**, 11.10.11-33 (2013).

74. P. Cingolani, A. Platts, L. Wang le, M. Coon, T. Nguyen, L. Wang, S. J. Land, X. Lu, D. M. Ruden, A program for annotating and predicting the effects of single nucleotide polymorphisms, SnpEff: SNPs in the genome of Drosophila melanogaster strain w1118; iso-2; iso-3. *Fly* **6**, 80-92 (2012).

Figures

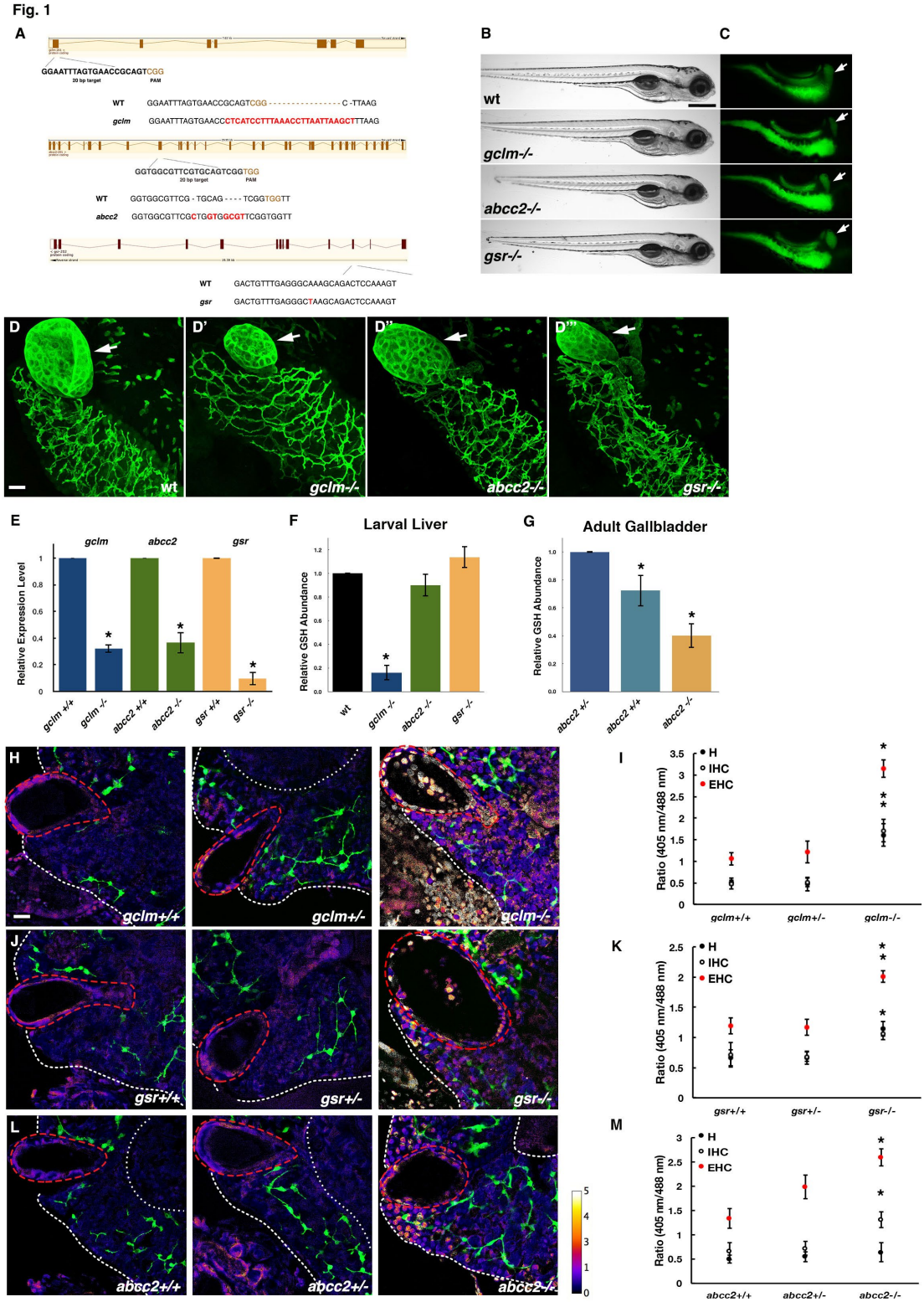

Fig. 1. Genetic disruption of glutathione metabolism genes in zebrafish differentially alter

EHC, IHC and hepatocyte basal redox status. (A) Schematic representation of the zebrafish *gclm* and *abcc2* loci with the CRISPR target site, protospacer adjacent motif, and WT and indel sequences. Nucleotide changes, confirmed by cDNA sequencing, are highlighted in red. Schematic representation of the *gsr*^{sa15125} mutant locus with the single nucleotide change highlighted in red. (B and C) Lateral bright field and fluorescent images of live 5 dpf WT, *gclm, abcc2, gsr* homozygous mutant larvae. Larvae were soaked in the fluorescent phospholipid Bodipy-C16 for 4 hours before imaging to evaluate the hepatobiliary function. (n=20 for each genotype). Arrow - gallbladder. Scale bars, 500 µm. (D) Confocal projections through the livers of 5 dpf WT, *gclm*, *abcc2*, and *gsr* homozygous mutant larvae immunostained with anti-Annexin A4 antibody showing normal extra-hepatic and intra-hepatic biliary morphology. Arrow - gallbladder. Scale bar, 20 µm. (E) Relative expression levels of the targeted transcripts in homozygous mutant larvae compared to WT siblings as determined by quantitative RT-PCR. *n* = 30 per genotype; *$p<1x10^{-5}$ by two-tailed unpaired student *t* test. (F) Hepatic GSH levels in homozygous mutant larvae compared with WT sibling controls (*n* = 15 dissected livers per genotype). *$p=1.23x10^{-6}$ by two-tailed unpaired student *t* test. (G) Relative GSH levels in gallbladders dissected from adult heterozygous and homozygous *abcc2*$^{-}$ mutant larvae compared with WT sibling controls (*n* = 9 per genotype). *p<0.02 per ANOVA with Tukey's multiple comparison test. All values are mean +/- standard errors of mean (SEM). WT, wildtype. (H, J, L) *In situ* measurement of basal glutathione redox potential. Representative composite confocal images through the livers of *gclm* (H), *gsr* (J), *abcc2* (L) bigenic mutant larvae *Tg* (*e1f: Grx1-roGFP*; *tp1:mCherry*). Glutathione redox status of EHC (gallbladder-dashed red circle), IHC, and hepatocytes was derived from the roGFP 405nm/488nm fluorescence excitation ratio. Color bar on right (a higher excitation ratio indicates a more oxidized environment). EHC and hepatocytes

localized by morphology. IHC localized by mCherry expression (pseudo-colored green to show location relative to hepatocytes). White dashed line - liver border. Scale bar, 10 μm. (I, K, M) Mean fluorescent 405 nm/488 nm excitation ratios in EHC, IHC, and hepatocytes for each genotype. *n* =10 larvae per genotype, means +/- SEM, *p<0.02 in comparison to WT EHC, IHC, or hepatocytes, respectively, per ANOVA with Tukey's multiple comparison test. EHC, extrahepatic cholangiocytes; IHC, intrahepatic cholangiocytes; H, hepatocytes.

Fig. 2

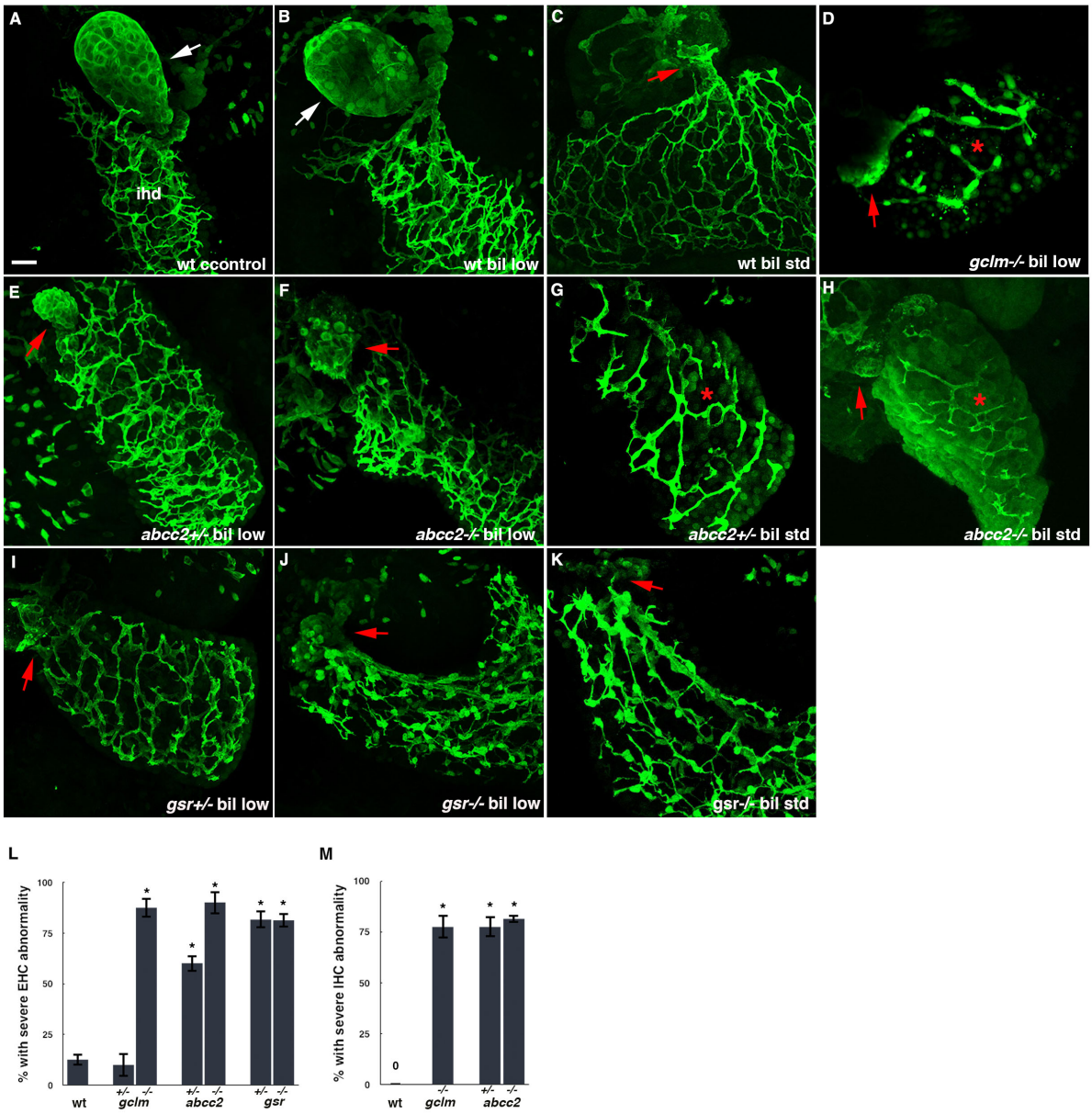

Fig. 2. Glutathione metabolism gene mutations differentially sensitize cholangiocytes to biliatresone. Confocal projections through the livers of 6 dpf WT (A-C), *gclm* (D), *abcc2* (E-H), *gsr* (I-K) mutant larvae exposed to low-dose or standard dose biliatresone for 24 hr. All larvae immunostained with anti-Annexin A4 antibody. White arrow – Gallbladder; red arrow – gallbladder remnant. * denotes liver with IHC injury. Scale bar, 20 µm. (L) Percentage of *gclm, abcc2*, *gsr* mutant larvae and their WT sibling controls with severe EHC abnormalities after low-

dose biliatresone exposure. (M) Percentage of *gclm, abcc2* mutant larvae and their WT siblings with IHC abnormalities after biliatresone exposure (either low-dose or standard dose). n = 30-36 per genotype per condition, means +/- SEM, *p<0.001 in comparison to WT control EHC or IHC, per ANOVA with Tukey's multiple comparison test. bil low, low-dose biliatresone; bil std, standard dose biliatresone; EHC, extrahepatic cholangiocytes, IHC, intrahepatic cholangiocytes; WT, wildtype.

Fig. 3

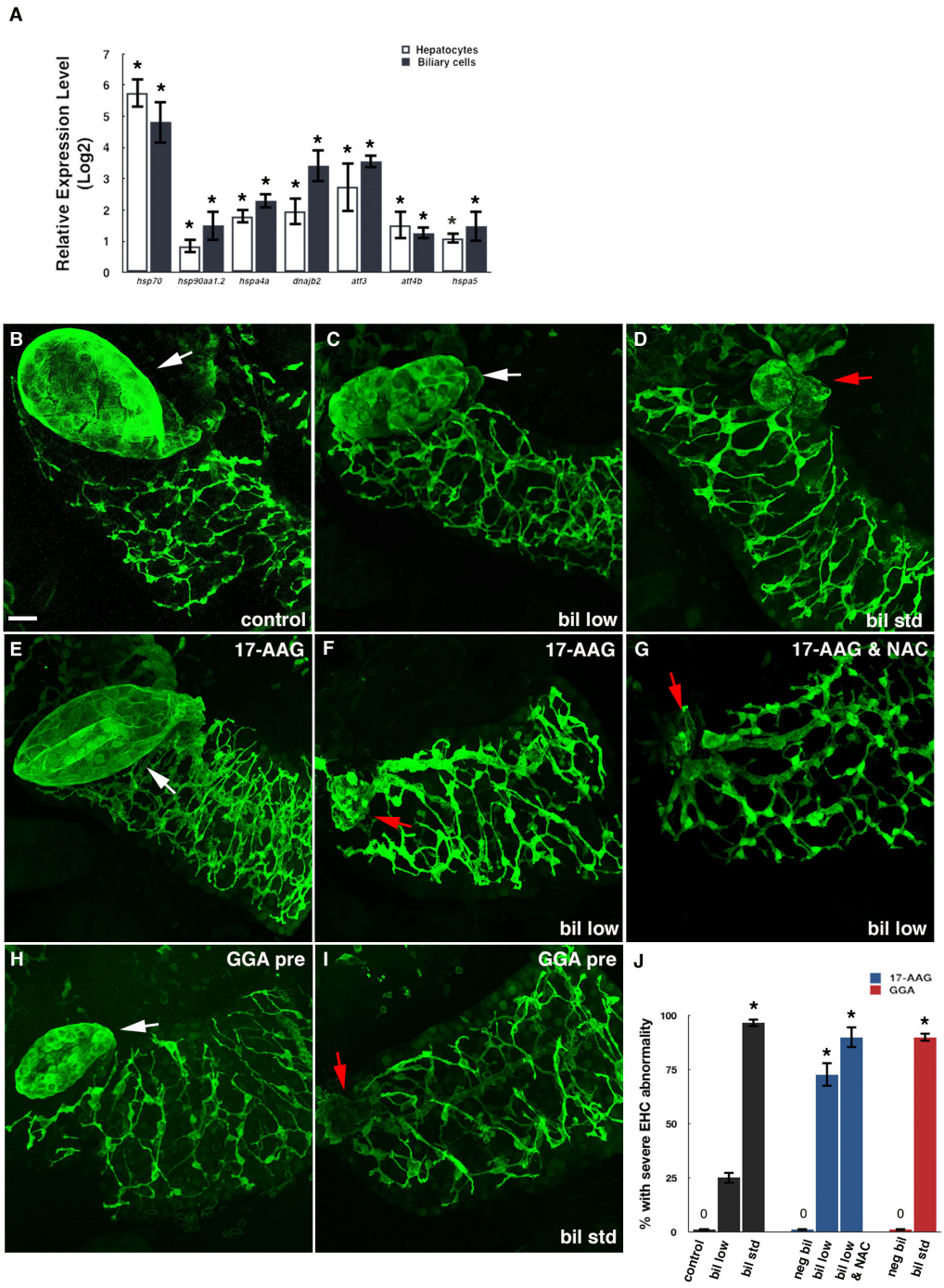

Fig. 3. Hsp90 inhibition sensitizes EHC to biliatresone. (A) Expression of heat shock response and unfolded protein response genes in biliatresone-treated larval hepatocytes and cholangiocytes *versus* DMSO-treated controls as determined by nCounter technology. means +/- SEM, *p<0.02

in comparison to DMSO-treated control larvae by two-tailed unpaired student *t* test. (B-I) Confocal projections through the livers of 6 dpf larvae immunostained with anti-Annexin A4 antibody. (B-D) WT control larva, and sibling larvae exposed to either low-dose, or standard dose biliatresone. (E-G) 6 dpf larvae exposed to 17-AAG alone, 17-AAG with low-dose biliatresone, or 17-AAG with low-dose biliatresone and NAC. (H-I) 6 dpf larvae exposed to GGA or GGA and standard dose biliatresone. All exposures for 24 hr. White arrow – Gallbladder; red arrow – gallbladder remnant. Scale bar, 20 μm. (J) Percentage of larvae exposed to biliatresone, biliatresone & 17-AAG, or biliatresone & GGA with severe EHC abnormalities. n = 30-32 per condition, mean +/- SEM, *$p<0.001$ in comparison to control larvae per ANOVA with Tukey's multiple comparison test. bil low, low-dose biliatresone; bil std, standard dose biliatresone; EHC, extrahepatic cholangiocytes, 17-AAG, 17-*N*-allylamino-17-demethoxygeldanamycin; GGA, geranylgeranyl acetate; NAC, N-acetylcysteine.

Fig. 4

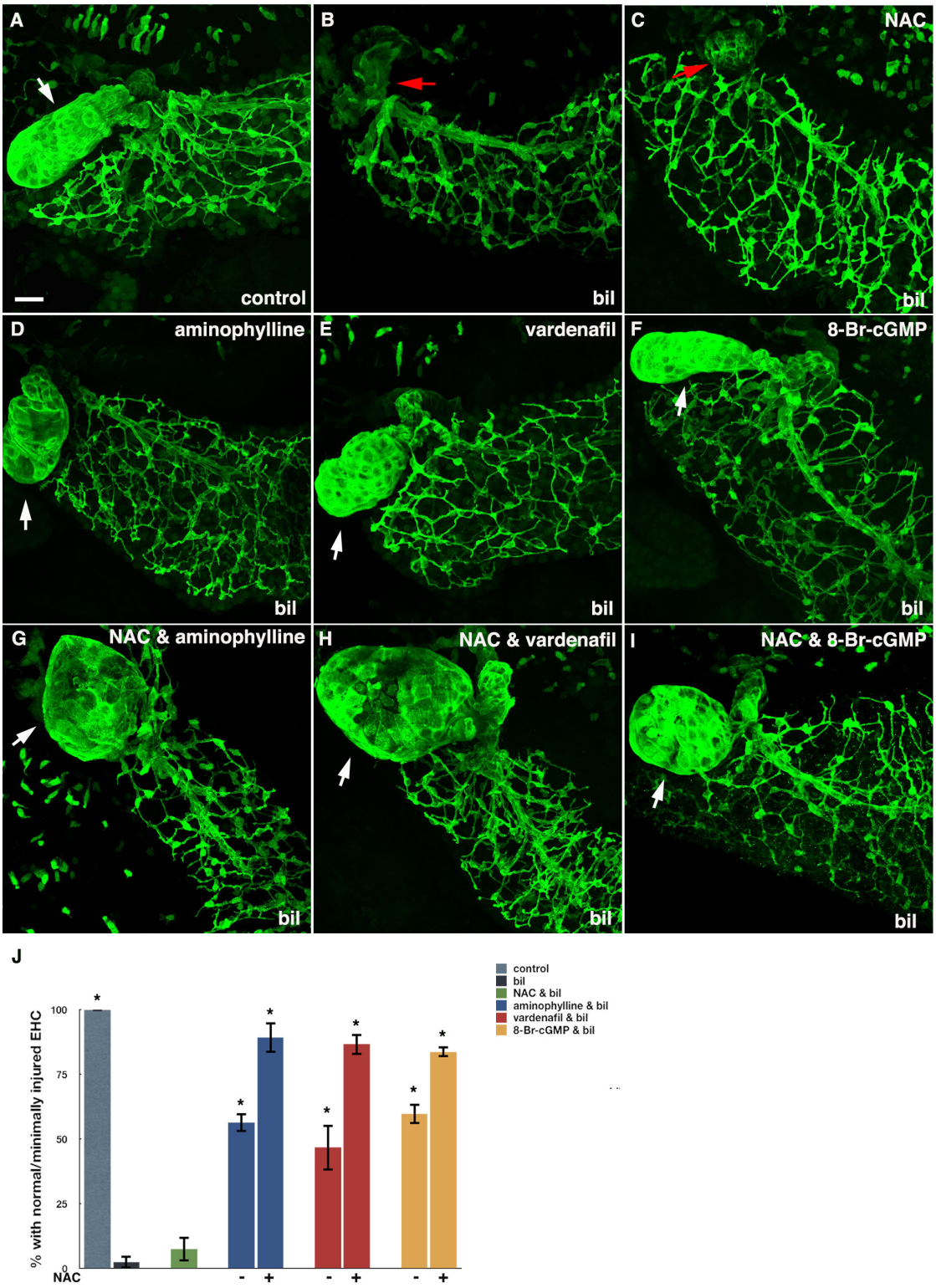

Fig. 4. Activation of cGMP signaling attenuates biliatresone-mediated EHC injury.

Confocal projections through the livers of 8 dpf larvae immunostained with anti-Annexin A4 antibody. (A-C) WT control larva, and WT larvae treated with standard dose biliatresone, or biliatresone and NAC. (D-F) Larvae treated with biliatresone and PDE inhibitors (aminophylline or vardenafil), or biliatresone and 8-Br-cGMP. (G-I) Larvae treated with biliatresone, PDE inhibitors and NAC, or biliatresone, 8-Br-cGMP and NAC. All exposures for 72 hr. White arrow – Gallbladder; red arrow – gallbladder remnant. Scale bar, 20 μm. (J) Percentage of biliatresone-treated larvae exposed to the indicated cGMP modulators with normal or minimally injured EHC. n = 30-36 per condition, mean +/- SEM, *$p<0.001$ in comparison to biliatresone-treated larvae per ANOVA with Tukey's multiple comparison test. bil, biliatresone; EHC, extrahepatic cholangiocytes; 8-Br-cGMP, 8-Bromoguanosine 3',5'-cyclic monophosphate; NAC, N-acetylcysteine.

Fig. 5

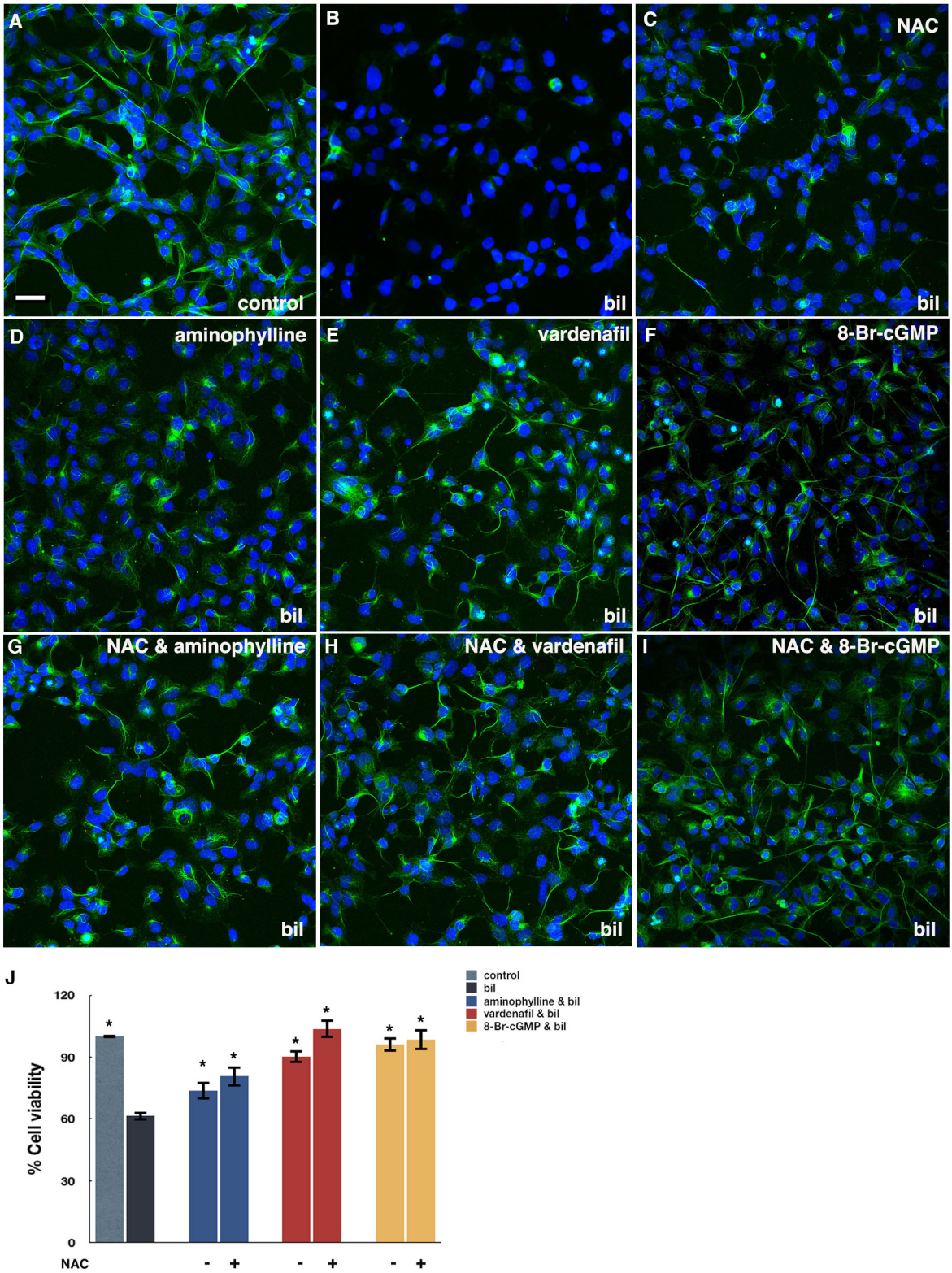

Fig. 5. Enhancing cGMP signaling reduces biliatresone toxicity in human cholangiocytes.

H69 cells immunostained with anti-acetylated tubulin antibody (green) with DAPI (blue) counterstain. (A) Control cells; (B-C) cells treated with standard dose biliatresone with and without NAC. (D-F) Cells treated with biliatresone and cGMP modulators (aminophylline, vardenafil, 8-Br-cGMP). (G-I) Cells treated with biliatresone, cGMP modulators and NAC. Scale bar, 10 μm. (J) Viability of biliatresone-treated H69 cells co-exposed to cGMP modulators with and without NAC as determined by MTS assay. Results are expressed as a percentage of control (DMSO-treated cells) ± SEM, *$p<0.001$ in comparison to biliatresone-treated H69 cells per ANOVA with Tukey's multiple comparison test. bil, biliatresone; 8-Br-cGMP, 8-Bromoguanosine 3',5'-cyclic monophosphate; NAC, N-acetylcysteine.

Fig. 6

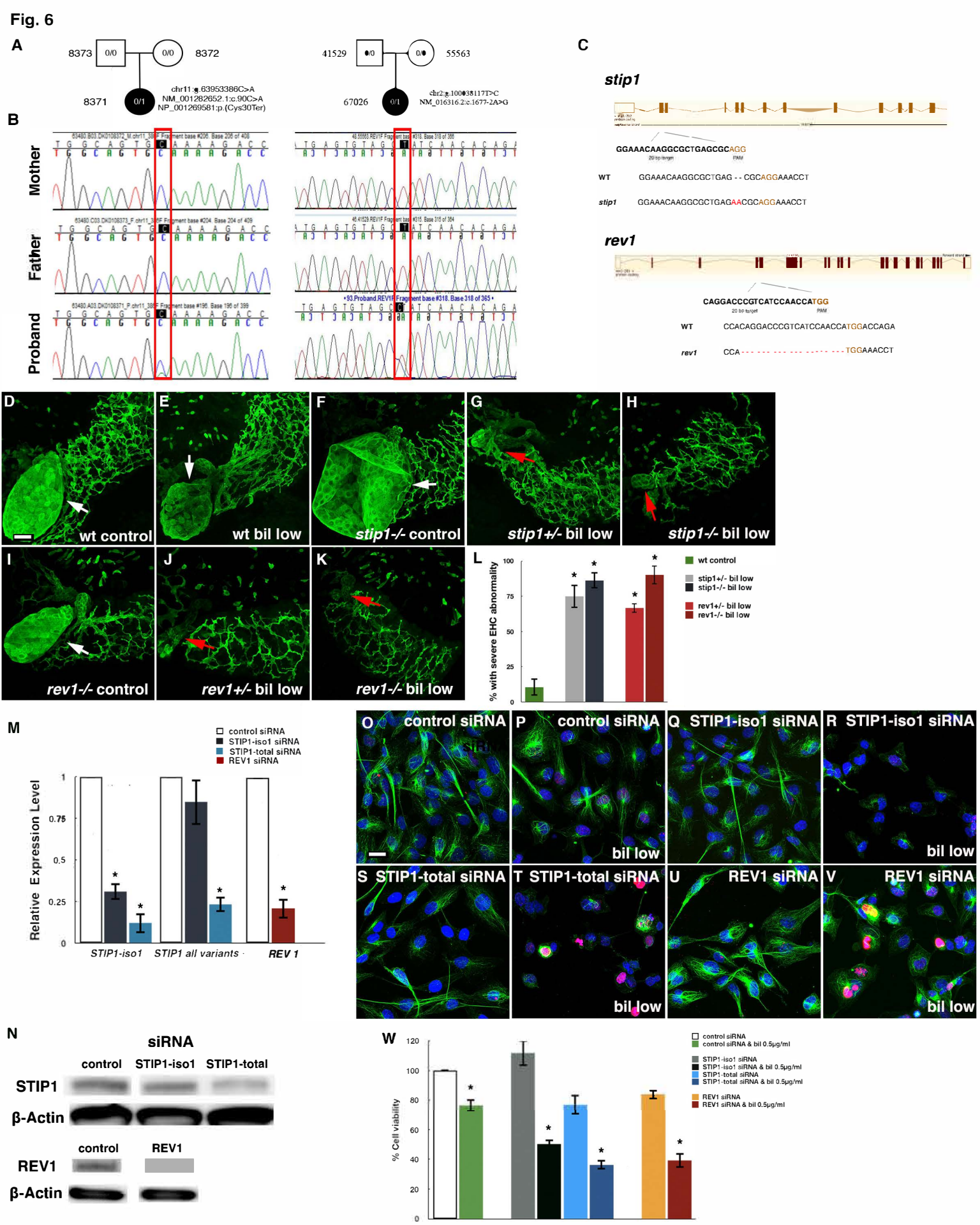
A
8373
0/0
0/0
8372
8371
0/1
chr11:g.63953386C>A
NM_001282652.1:c.90C>A
NP_001269581:p.(Cys30Ter)
41529
0/0
0/0
55563
67026
0/1
chr2:g.100035117T>C
NM_016316.2:c.1677-2A>G
B
Mother
Father
Proband
C
stip1
GGAAACAAGGCGCTGAGCGCAGG
20 bp target
PAM
WT GGAAACAAGGCGCTGAG - - CGCAGGAAACCT
stip1 GGAAACAAGGCGCTGAGAACGCAGGAAACCT
rev1
CAGGACCCGTCATCCAACCATGG
20 bp target
PAM
WT CCACAGGACCCGTCATCCAACCATGGACCAGA
rev1 CCA - - - - - - - - - - - - - - - - - - TGGAAACCT
D wt control
E wt bil low
F stip1-/- control
G stip1+/- bil low
H stip1-/- bil low
I rev1-/- control
J rev1+/- bil low
K rev1-/- bil low
L
% with severe EHC abnormality
100
75
50
25
0
wt control
stip1+/- bil low
stip1-/- bil low
rev1+/- bil low
rev1-/- bil low
M
control siRNA
STIP1-iso1 siRNA
STIP1-total siRNA
REV1 siRNA
Relative Expression Level
1
0.75
0.5
0.25
0
STIP1-iso1
STIP1 all variants
REV 1
O control siRNA
P control siRNA
bil low
Q STIP1-iso1 siRNA
R STIP1-iso1 siRNA
bil low
S STIP1-total siRNA
T STIP1-total siRNA
bil low
U REV1 siRNA
V REV1 siRNA
bil low
N
siRNA
control
STIP1-iso1
STIP1-total
STIP1
β-Actin
control
REV1
REV1
β-Actin
W
% Cell viability
120
100
80
60
40
20
0
control siRNA
control siRNA & bil 0.5μg/ml
STIP1-iso1 siRNA
STIP1-iso1 siRNA & bil 0.5μg/ml
STIP1-total siRNA
STIP1-total siRNA & bil 0.5μg/ml
REV1 siRNA
REV1 siRNA & bil 0.5μg/ml

Fig. 6. Stip1 and Rev1 disruption sensitizes zebrafish and human cholangiocytes to biliatresone. (A) Germline *STIP1* and *REV1* variants in two children with BA. (B) Sanger sequencing traces confirming that the variants are *de novo* in the proband (red box). (C) Schematic representation of the zebrafish *stip1* and *rev1* loci with the CRISPR target sites, protospacer adjacent motif, and WT and indel sequences. (D-K) Confocal projections through the livers of 6 dpf larvae immunostained with anti-Annexin A4 antibody: wt larvae (D-E) and *stip1* (F-H), *rev1* (), *rev1*$^{-/-}$ (I-K) larvae treated with DMSO *versus* low-dose biliatresone for 24 hr. White arrow – Gallbladder; red arrow – gallbladder remnant. (L) Percentage of wt, *stip1* and *rev1* larvae with severe EHC abnormalities after exposure to low-dose biliatresone. n = 30 per genotype and condition, mean +/- SEM, *p<0.001 in comparison to control larvae per ANOVA with Tukey's multiple comparison test. (M) mRNA levels of *STIP1 isoform 1,* total *STIP1, rev1* expression in H69 cells 24 hr post transfection with negative control siRNA, STIP1-isoform 1 siRNA, STIP1-total siRNA, REV1 siRNA as determined by qRT-PCR. n = 3 per condition, mean +/- SEM, *p<0.05 in comparison to control cells per ANOVA with Tukey's multiple comparison test. (N) Western blot showing protein levels of STIP1 and REV1 extracted from H69 cells 48 hr post transfection with negative control siRNA, STIP1-isoform 1 siRNA, STIP1-total siRNA, REV1 siRNA. (O-V) H69 cells immunostained with anti-acetylated tubulin antibody (green), anti-yH2AX (red) and DAPI (blue) counter stain. Cells treated with negative control siRNA (O) or negative control siRNA followed by low-dose biliatresone (P). Cells transfected with STIP1-isoform 1 siRNA (Q), STIP1-total siRNA (S) REV1 siRNA (U) followed by low-dose biliatresone (R, T, V). Scale bar, 10 µm. (w) Bar graphs of relative cell viability of H69 cells transfected with control siRNA, STIP1-

iso1 siRNA, STIP1-total siRNA, or REV1-siRNA followed by exposure to low-dose biliatresone as determined by MTT assay. Results are expressed as a percentage of control ± SEM, *$p<0.001$ in comparison to H69 cells treated with control siRNA per ANOVA with Tukey's multiple comparison test. bil low, low-dose biliatresone; EHC, extrahepatic cholangiocytes; STIP1-iso1, STIP1 isoform 1.

Fig.7

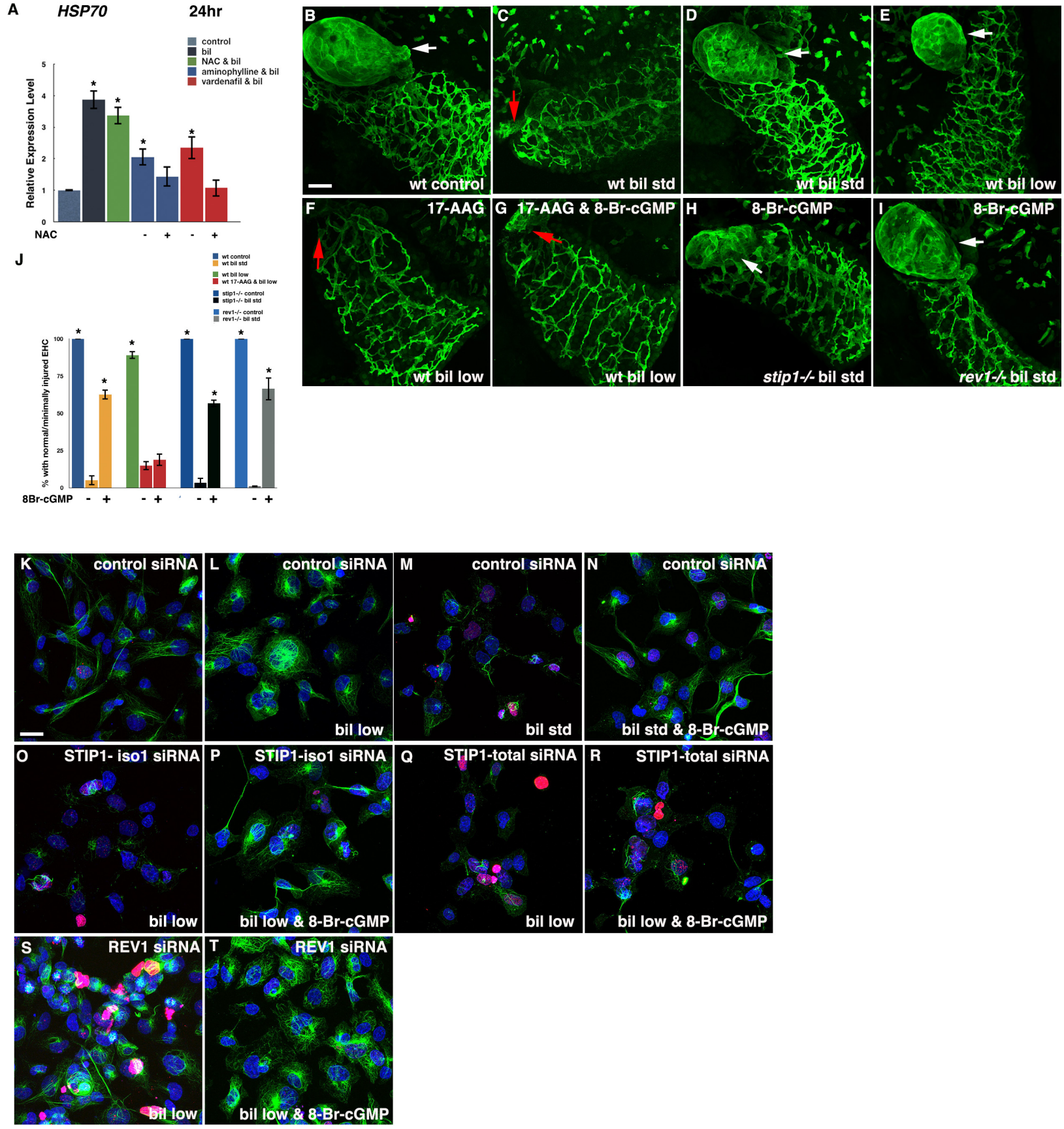
A
HSP70
24hr
control
bil
NAC & bil
aminophylline & bil
vardenafil & bil
Relative Expression Level
NAC
B
wt control
C
wt bil std
D
wt bil std
E
wt bil low
F
17-AAG
wt bil low
G
17-AAG & 8-Br-cGMP
wt bil low
H
8-Br-cGMP
stip1-/- bil std
I
8-Br-cGMP
rev1-/- bil std
J
wt control
wt bil std
wt bil low
wt 17-AAG & bil low
stip1-/- control
stip1-/- bil std
rev1-/- control
rev1-/- bil std
% with normal/minimally injured EHC
8Br-cGMP
K
control siRNA
L
control siRNA
bil low
M
control siRNA
bil std
N
control siRNA
bil std & 8-Br-cGMP
O
STIP1- iso1 siRNA
bil low
P
STIP1-iso1 siRNA
bil low & 8-Br-cGMP
Q
STIP1-total siRNA
bil low
R
STIP1-total siRNA
bil low & 8-Br-cGMP
S
REV1 siRNA
bil low
T
REV1 siRNA
bil low & 8-Br-cGMP

Fig 7. cGMP rescue of biliatresone toxicity is dependent on heat shock proteostasis. (A) Relative HSP70 expression in H69 cells 24 hr post-treatment with DMSO (control), biliatresone, biliatresone and NAC, biliatresone and PDE inhibitors (aminophylline, vardenafil) on their own or combined with NAC. n = 3 replicates per condition, mean +/- SEM, *p<0.001 in comparison to control cells per ANOVA with Tukey's multiple comparison test. (B-I) Confocal projections through livers of biliatresone-treated WT, *stip1*, or *rev1* larvae immunostained with Annexin-A4 antibody comparing the effect of 8-Br-cGMP. White arrow – Gallbladder; red arrow – gallbladder remnant. Scale bar, 20 μm. (J) Bar graph showing the percentage of WT, *stip1*, or *rev1* larvae larvae treated with biliatresone with normal or minimally injured EHC following co-treatment with 8-Br-cGMP. n = 30 per genotype per condition, mean +/- SEM, *p<0.001 in comparison to larvae treated with standard-dose biliatresone per ANOVA with Tukey's multiple comparison test. (K-T) H69 cells immunostained with anti-acetylated tubulin antibody (green), anti-yH2AX (red) and DAPI (blue) counterstain. Cells treated with negative control siRNA (K) or negative control siRNA followed by biliatresone with or without 8-Br-cGMP (L-N). Cells transfected with STIP1-isoform 1 siRNA (O, P), STIP1-total siRNA (Q, R), or REV1 siRNA (S, T) followed by low-dose biliatresone with or without 8-Br-cGMP. Scale bar, 10 μm. bil low, low-dose biliatresone; bil std, standard dose biliatresone; EHC, extrahepatic cholangiocytes, 17-AAG, 17-N-allylamino-17-demethoxygeldanamycin; 8-Br-cGMP, 8-Bromoguanosine 3',5'-cyclic monophosphate, STIP1-iso1, STIP1 isoform 1.

Fig. 8

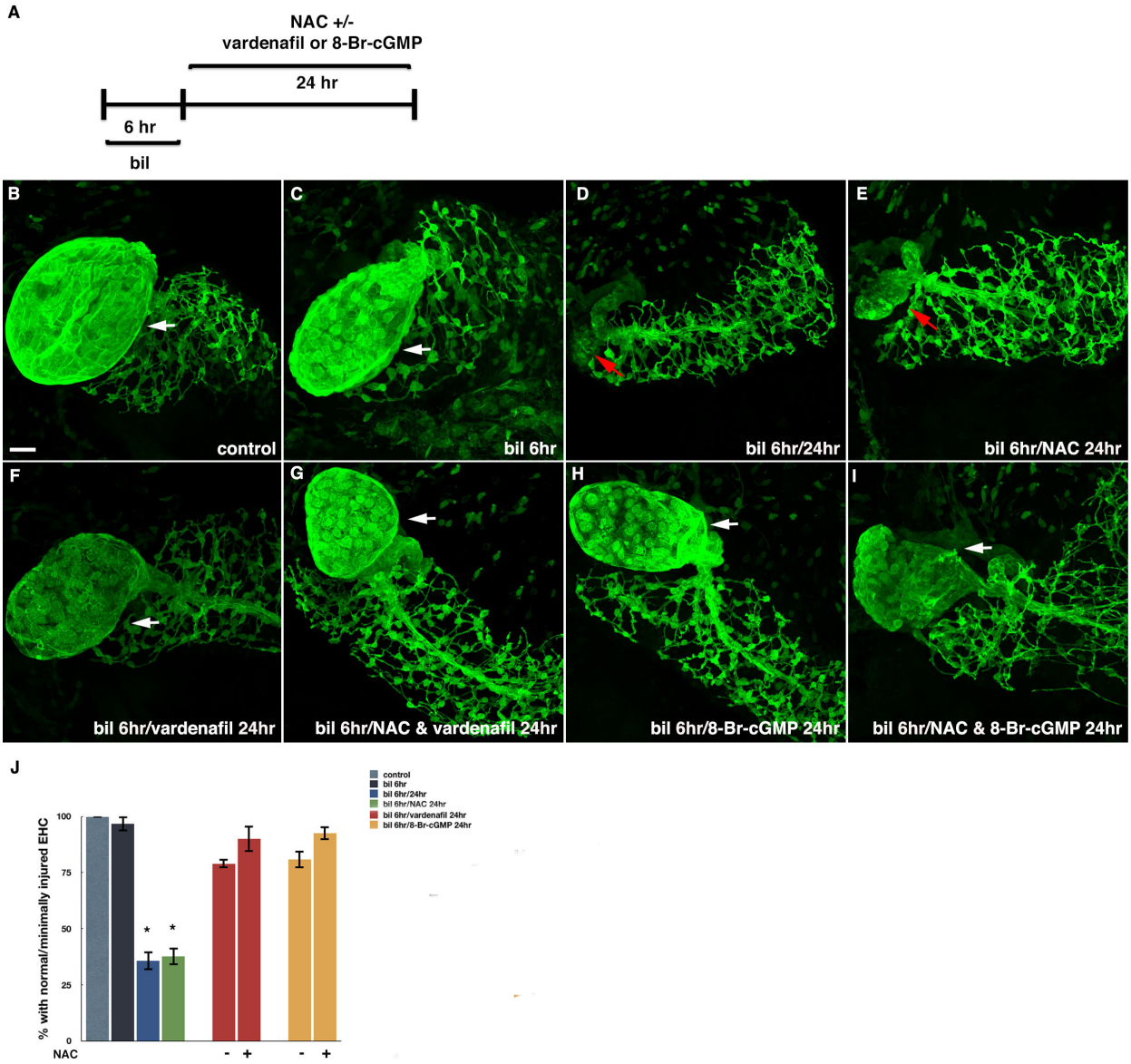

Fig. 8 Short term biliatresone exposure triggers EHC injury that is blocked by cGMP. (A) Experimental scheme depicting treatment of zebrafish larvae with standard dose biliatresone for 6 hr, followed by incubation with cGMP modulators (vardenafil or 8-Br-cGMP) with and without NAC for 24 hr. (B-I) Confocal projections through the livers of 5-6 dpf larvae immunstained with anti-Annexin A4 antibody. (B) Control larva, (C-D) Larvae exposed to biliatresone alone imaged 6 hr and 24 hr post treatment initiation, respectively. (E-I) Larvae treated with biliatresone for 6 hr

followed by treatment with NAC (E); vardenafil +/- NAC (F-G); 8-Br-cGMP +/- NAC (H-I) for 24 hr. Scale bar, 20 μm. (J) Percentage of larvae exhibiting normal or minimally injured EHC after biliatresone exposure for 6 hr followed by treatments with NAC/cGMP modulators. *n* = 30-35 per condition, mean +/- SEM, *p<0.001 in comparison to control larvae per ANOVA with Tukey's multiple comparison test. bil, biliatresone; EHC, extrahepatic cholangiocytes; 8-Br-cGMP, 8-Bromoguanosine 3',5'-cyclic monophosphate; NAC, N-acetylcysteine.